The thesis entitled "**Synthesis and Biological Studies of Pyrazole, Nicotinaldehyde Based Heterocyclic Compounds and Development of Novel Approach for Pyrazoles and Quinazolines**" is divided into three parts, part-A, part-B, and part-C.

**Part-A**: Part-A represents the chapter-I

**Chapter-I**: The present chapter describes the "Synthesis, anti-bacterial and anti-inflammatory activities of pyrazole based heterocyclic compounds."

**Part-B**: Part-B divided into two chapters, chapter-I and chapter-II.

**Chapter-II**: The present chapter describes the "Synthesis and anti-cancer activity of pyridinylchalcones and chromanones."

**Chapter-III**: Chapter-III subdivided into two sections, section-A and section-B.

**Section-A**: The present section describes the "Synthesis of pyridinyl triazolylisonicotinohydrazides and their *anti-mycobacterial* activity."

**Section-B**: The present section describes the "Synthesis and biological activities of nicotinaldehyde based azlactones."

**Part-C**: Part-C divided into two chapters, chapter-IV and chapter-V.

**Chapter-IV**: The present chapter describes the "Synthesis of benzimidazoles, pyrazolones and pyrazoles."

**Chapter-V**: The present chapter describes "A selective three-component, one-pot approach for the synthesis of 1,2-dihydroquinazolines and quinazolines.

## PART-A, CHAPTER-I

**Synthesis, anti-bacterial and anti-inflammatory activities of pyrazole based heterocyclic compounds.**

The present chapter describes the preparation of three series of compounds namely I) pyrazolyl 1,2,3-triazolyl alcohols **8a-h**, II) pyrazolyl 1,2,3-triazoles **10a-p** and III) pyrazolyl 1,2,3-triazolyl carboxylates **12a-l**. The prepared compounds **8a-h, 10a-p** and **12a-l** were evaluated for their anti-microbial and anti-inflammatory activities [TNF-α and IL-6 (*in vitro*) and LPS induced mice (*in vivo*)]. Docking studies were performed for the identified active compounds.

**Preparation of pyrazolyltriazoles** (**8a-h, 10a-p** and **12a-l**).

Condensation of acetophenones **1a-h** with phenylhydrazine hydrochlorides **2a-h** in the presence of acetic acid at room temperature provided the phenylhydrazones **3a-h** (**Scheme 1**). Vilsmeier-Haack reaction of **3a-h** in the presence of DMF and $POCl_3$ afforded pyrazole carboxaldehydes **4a-h.** $NaBH_4$ reduction of carboxaldehydes **4a-h** provided the alcohols **5a-h**. Alcohols **5a-h** were converted to azides **6a-h** in the presence of DPPA and DBU. The cycloaddition reaction of azides **6a-h** with propargyl alcohol **7** in the presence of $CuSO_4.5H_2O$ and sodium ascorbate in aqueous alcohol medium provided the pyrazolyl-1*H*-1,2,3-triazolyl alcohols **8a-h** (**Scheme 1**).

Scheme 2 depicts the cycloaddition reaction of azides **6a-f** with phenyl acetylenes **9a-k** under optimized conditions provided the pyrazolyl-1*H*-1,2,3-triazoles **10a-p**. Next, the cycloaddition carried out with dimethyl, diethyl acetylenedicarboxylates **11a-b**. This provided the pyrazolyl-1*H*-1,2,3-triazolyl carboxylates **12a-l** (**Scheme 3**). Thus prepared compounds **8a-h**, **10a-p** and **12a-l** are unknown and well characterized by spectral data.

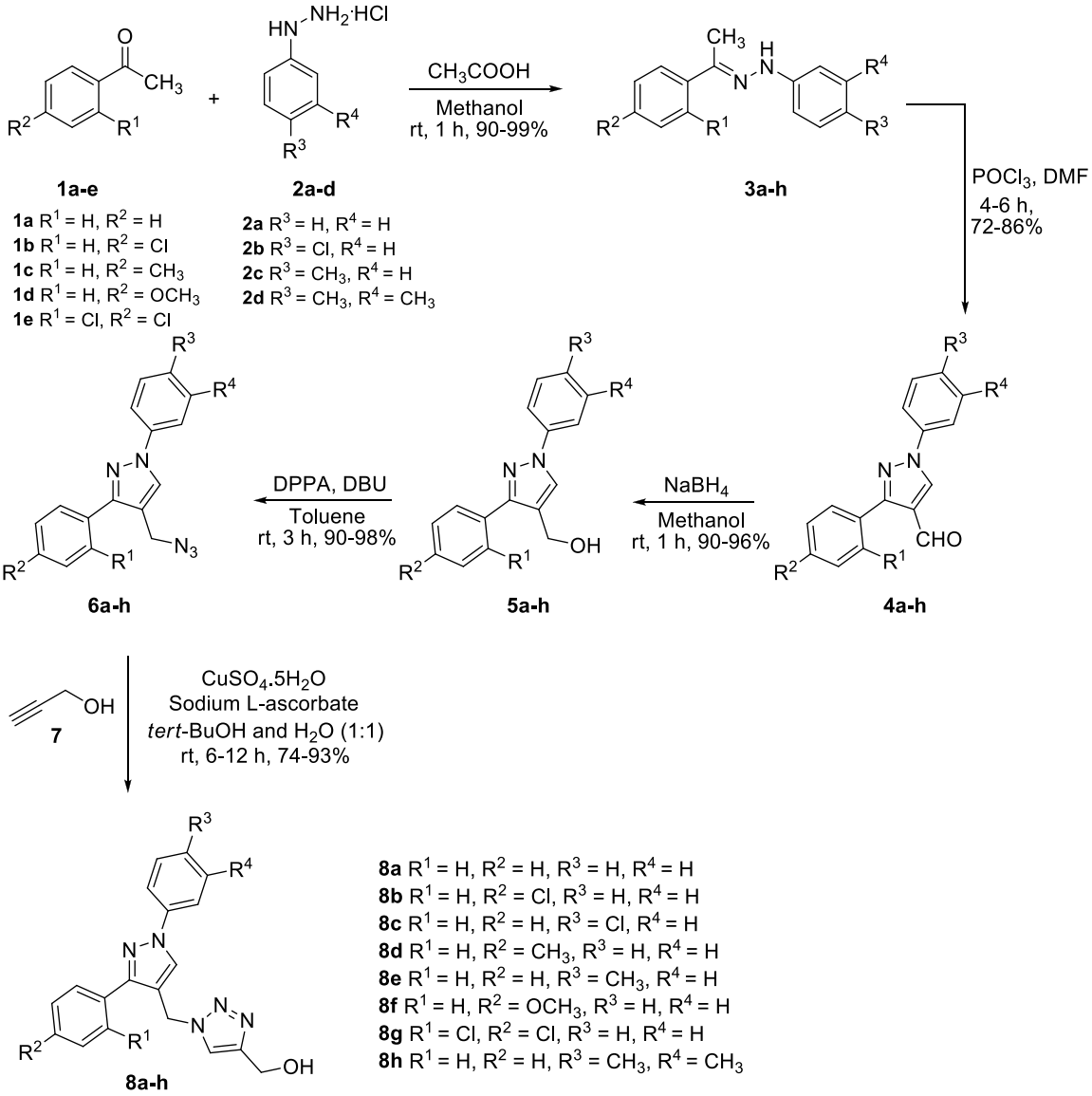


**1a** $R^1$ = H, $R^2$ = H
**1b** $R^1$ = H, $R^2$ = Cl
**1c** $R^1$ = H, $R^2$ = $CH_3$
**1d** $R^1$ = H, $R^2$ = $OCH_3$
**1e** $R^1$ = Cl, $R^2$ = Cl

**2a** $R^3$ = H, $R^4$ = H
**2b** $R^3$ = Cl, $R^4$ = H
**2c** $R^3$ = $CH_3$, $R^4$ = H
**2d** $R^3$ = $CH_3$, $R^4$ = $CH_3$

**8a** $R^1$ = H, $R^2$ = H, $R^3$ = H, $R^4$ = H
**8b** $R^1$ = H, $R^2$ = Cl, $R^3$ = H, $R^4$ = H
**8c** $R^1$ = H, $R^2$ = H, $R^3$ = Cl, $R^4$ = H
**8d** $R^1$ = H, $R^2$ = $CH_3$, $R^3$ = H, $R^4$ = H
**8e** $R^1$ = H, $R^2$ = H, $R^3$ = $CH_3$, $R^4$ = H
**8f** $R^1$ = H, $R^2$ = $OCH_3$, $R^3$ = H, $R^4$ = H
**8g** $R^1$ = Cl, $R^2$ = Cl, $R^3$ = H, $R^4$ = H
**8h** $R^1$ = H, $R^2$ = H, $R^3$ = $CH_3$, $R^4$ = $CH_3$

**Scheme 1**

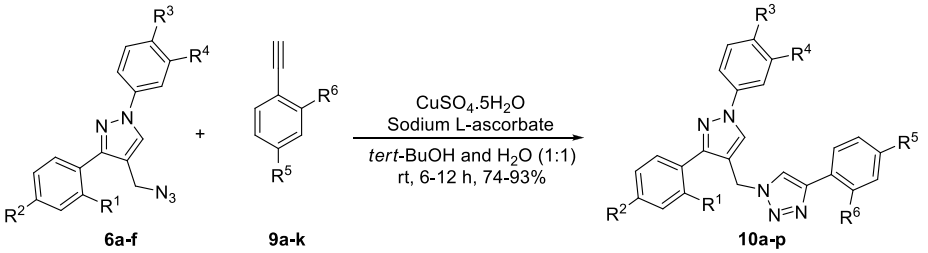


**6a-f** **9a-k** **10a-p**

**10a** $R^1$ = H, $R^2$ = H, $R^3$ = H, $R^4$ = H, $R^5$ = H, $R^6$ = H
**10b** $R^1$ = H, $R^2$ = Cl, $R^3$ = H, $R^4$ = H, $R^5$ = H, $R^6$ = H
**10c** $R^1$ = H, $R^2$ = H, $R^3$ = Cl, $R^4$ = H, $R^5$ = H, $R^6$ = H
**10d** $R^1$ = H, $R^2$ = $CH_3$, $R^3$ = H, $R^4$ = H, $R^5$ = H, $R^6$ = H
**10e** $R^1$ = H, $R^2$ = H, $R^3$ = $CH_3$, $R^4$ = H, $R^5$ = H, $R^6$ = H
**10f** $R^1$ = H, $R^2$ = $OCH_3$, $R^3$ = H, $R^4$ = H, $R^5$ = H, $R^6$ = H
**10g** $R^1$ = H, $R^2$ = H, $R^3$ = H, $R^4$ = H, $R^5$ = H, $R^6$ = $CF_3$
**10h** $R^1$ = H, $R^2$ = H, $R^3$ = H, $R^4$ = H, $R^5$ = $CF_3$, $R^6$ = $CF_3$
**10i** $R^1$ = H, $R^2$ = H, $R^3$ = H, $R^4$ = H, $R^5$ = $NH_2$, $R^6$ = H
**10j** $R^1$ = H, $R^2$ = H, $R^3$ = H, $R^4$ = H, $R^5$ = $N(CH_3)_2$, $R^6$ = H
**10k** $R^1$ = H, $R^2$ = H, $R^3$ = H, $R^4$ = H, $R^5$ = F, $R^6$ = H
**10l** $R^1$ = H, $R^2$ = H, $R^3$ = H, $R^4$ = H, $R^5$ = Cl, $R^6$ = H
**10m** $R^1$ = H, $R^2$ = H, $R^3$ = H, $R^4$ = H, $R^5$ = Br, $R^6$ = H
**10n** $R^1$ = H, $R^2$ = H, $R^3$ = H, $R^4$ = H, $R^5$ = $CH_3$, $R^6$ = H
**10o** $R^1$ = H, $R^2$ = H, $R^3$ = H, $R^4$ = H, $R^5$ = $OCH_3$, $R^6$ = H
**10p** $R^1$ = H, $R^2$ = H, $R^3$ = H, $R^4$ = H, $R^5$ = $OCH_3$, $R^6$ = $CH_3$

## Scheme 2

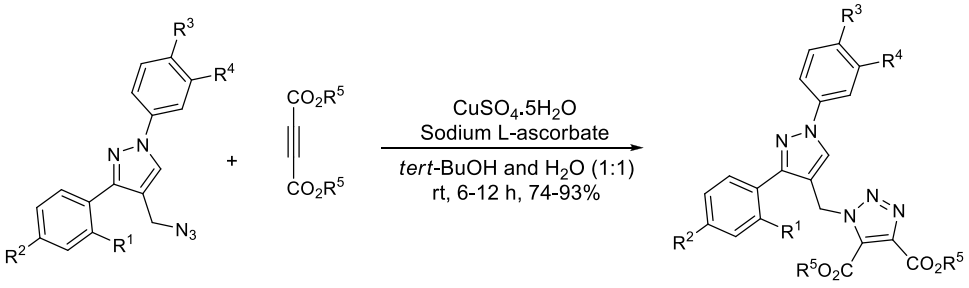


**6a-f** **11a-b** **12a-l**

**12a** $R^1$ = H, $R^2$ = H, $R^3$ = H, $R^4$= H, $R^5$ = $CH_3$
**12b** $R^1$ = H, $R^2$ = Cl, $R^3$ = H, $R^4$= H, $R^5$ = $CH_3$
**12c** $R^1$ = H, $R^2$ = H, $R^3$ = Cl, $R^4$= H, $R^5$ = $CH_3$
**12d** $R^1$ = H, $R^2$ = $CH_3$, $R^3$ = H, $R^4$= H, $R^5$ = $CH_3$
**12e** $R^1$ = H, $R^2$ = H, $R^3$ = $CH_3$, $R^4$= H, $R^5$ = $CH_3$
**12f** $R^1$ = H, $R^2$ = $OCH_3$, $R^3$ = H, $R^4$= H, $R^5$ = $CH_3$
**12g** $R^1$ = H, $R^2$ = H, $R^3$ = H, $R^4$= H, $R^5$ = $C_2H_5$
**12h** $R^1$ = H, $R^2$ = Cl, $R^3$ = H, $R^4$= H, $R^5$ = $C_2H_5$
**12i** $R^1$ = H, $R^2$ = H, $R^3$ = Cl, $R^4$= H, $R^5$ = $C_2H_5$
**12j** $R^1$ = H, $R^2$ = $CH_3$, $R^3$ = H, $R^4$= H, $R^5$ = $C_2H_5$
**12k** $R^1$ = H, $R^2$ = H, $R^3$ = $CH_3$, $R^4$= H, $R^5$ = $C_2H_5$
**12l** $R^1$ = H, $R^2$ = $OCH_3$, $R^3$ = H, $R^4$= H, $R^5$ = $C_2H_5$

## Scheme 3

***In vitro* anti-microbial activity**

The *in vitro* data of anti-microbial activity, minimum inhibitory concentration (MIC) and minimum bactericidal concentration (MBC) of all the synthesized compounds (**5a-h**, **6a-h**, **8a-h**, **10a-p** and **12a-l)** presented in Table 1. The *in vitro* anti-bacterial activity of compounds were tested against two Gram-positive organisms (*Micrococcus luteus* and *Staphylococcus aureus*) and two Gram-negative organisms (*Salmonella typhi* and *Salmonella paratyphi*) by agar well plate method and compared with streptomycin. The *in vitro* anti-fungal activity of compounds (**5a-h**, **6a-h, 8a-h**, **10a-p** and **12a-l)** were tested by agar plate method against two fungal strains (*Aspergillus niger* and *Aspergillus fumigates*) and compared with fluconazole. The MIC and MBC studies were performed by using tube dilution.

The chloro pyrazolyl alcohol **5c** and pyrazolyl triazole alcohol **8f** displayed better anti-bacterial activity (26.5 and 26 mm zone of inhibition) against *M.luteus* in comparison with standard (22.5 mm). Compound **5c** is the most potent compound [MIC value is 3.9 and 7.81µg/ml] against *M.luteus* when compared to streptomycin [6.25 µg/ml, MIC and MBC).

**Table 1.** Anti-bacterial activity of the compounds **5a-h** and **8a-h**.

| Compound* | Zone of inhibition in mm (MIC, MBC [µg/ml]) | | | |
|---|---|---|---|---|
| | Gram positive Bacteria | | Gram negative Bacteria | |
| | *M. luteus* | *S. aureus* | *S. typhi* | *S. paratyphi* |
| **5a** | -- | -- | 11.5 ± 0.71 | 14 ± 0.00 |
| **5b** | -- | -- | -- | 12 ± 0.00 |
| **5c** | 26.5 ± 0.71 (3.9, 7.81) | -- | 21.5 ± 0.71 (62.5, 125) | 18 ± 0.00 (31.25, 62.5) |
| **5d** | 16.5 ± 0.71 | -- | 19 ± 0.00 | 14 ± 0.00 |
| **5e** | -- | -- | 17 ± 1.41 | 12.5 ± 0.71 |
| **5f** | -- | -- | -- | 11.5 ± 0.71 |
| **5g** | -- | -- | 13.5 ± 0.71 | 11.5 ± 0.71 |
| **5h** | -- | -- | 14.5 ± 0.71 | 12 ± 0.00 |
| **8a** | -- | -- | -- | 12.5 ± 0.71 |
| **8b** | -- | -- | -- | 15 ± 0.00 |
| **8c** | 11.5 ± 0.71 | -- | 19.5 ± 0.71 | 16.5 ± 0.71 |
| **8d** | -- | -- | 15 ± 0.00 | 14 ± 0.00 |
| **8e** | -- | -- | 19 ± 0.00 | 11.5 ± 0.71 |
| **8f** | 26 ± 0.00 (125, 125) | -- | 16 ± 0.00 (62.5, 125) | 19 ± 0.00 (62.5, 62.5) |
| **8g** | -- | -- | 14 ± 1.41 | 17 ± 0.00 |
| **8h** | -- | -- | 15.5 ± 0.71 | -- |
| **Streptomycin** | 22.5 ± 0.71 (6.25, 6.25) | 20.3±0.57 | 27 ± 1.41 (6.25, 6.25) | 30 ± 0.00 (6.25, 6.25) |

*Compounds **6a-h**, **10a-p** and **12a-l** were not shown activity; hence they have not incorporated.

### *In vitro* anti-inflammatory activity

The *in vitro* anti-inflammatory activity of compounds **5a-h**, **6a-h**, **8a-h**, **10a-p** and **12a-l** were tested by using protein (egg albumin) denaturation method along with the standard drug, diclofenac sodium (**Table 2**). While LPS-induced TNF-α and IL-6 (based on enzyme-linked immunosorbent assay (ELISA) was carried out for those compounds which revealed better activity profile and compared with Rolipram (**Table 3**). Analysis of the structure activity relationship of compounds **5a-h** denoted $IC_{50}$ in the range of 54.21 to 105.45 µg/ml with respect to *in vitro* protein denaturation profile. The compound with chlorine substitution (**5c**, $IC_{50}$ 54.21 µg/ml) at *N*-aryl displayed equipotency with respect to the standard compound ($IC_{50}$ 53.70 µg/ml; **Table-2**).

Addition of triazole moiety to pyrazolyl derivative (**8a-h**) denoted $IC_{50}$ in the range of 58.00-128.89 µg/ml. Among these, the compound **8e** showed similar trend as that of

**5a-b** and **5h**. Comparing the activity profile of **5f** and **8f** (both have the methoxy substitution) with triazole moiety (**8f**) improved the activity (**Table 2**).

**Table 2.** Anti-inflammatory activity of the compounds **5a-h** and **8a-h** based on protein denaturation method.

| Compound* | Egg Albumin | | |
|---|---|---|---|
| | % inhibition | | $IC_{50}$ (µg/ml) |
| | 50 (µg/ml) | 100 (µg/ml) | |
| **5a** | 75.86 ± 0.17 | 87.93 ± 0.87 | 56.86 ± 0.76 |
| **5b** | 67.24 ± 0.44 | 83.62 ± 0.46 | 59.79 ± 0.34 |
| **5c** | 76.72 ± 0.89 | 92.24 ± 0.78 | 54.21 ± 0.87 |
| **5d** | 60.34 ± 0.43 | 81.90 ± 0.83 | 61.05 ± 0.65 |
| **5e** | 40.52 ± 0.72 | 68.10 ± 0.33 | 73.42 ± 0.54 |
| **5f** | 15.52 ± 0.85 | 47.41 ± 0.59 | 105.45 ± 0.85 |
| **5g** | 60.34 ± 0.58 | 80.17 ± 0.87 | 62.37 ± 0.43 |
| **5h** | 66.38 ± 0.22 | 83.62 ± 0.53 | 59.79 ± 0.12 |
| **8a** | 10.34 ± 0.89 | 38.79 ± 0.21 | 128.89 ± 0.74 |
| **8b** | 49.14 ± 0.47 | 73.28 ± 0.79 | 68.24 ± 0.32 |
| **8c** | 55.17 ± 0.78 | 78.45 ± 0.77 | 63.74 ± 0.84 |
| **8d** | 21.55 ± 0.64 | 38.79 ± 0.98 | 128.89 ± 0.75 |
| **8e** | 66.38 ± 0.95 | 83.62 ± 0.67 | 59.79 ± 0.39 |
| **8f** | 68.97 ± 0.44 | 86.21 ± 0.34 | 58.00 ± 0.71 |
| **8g** | 50.86 ± 0.25 | 76.72 ± 0.51 | 65.17 ± 0.82 |
| **8h** | 46.55 ± 0.77 | 77.59 ± 0.87 | 64.44 ± 0.55 |
| **Diclofenac sodium** | 66.38 ± 0.06 | 93.10 ± 0.12 | 53.70 ± 0.24 |

*Compounds **6a-h**, **10a-p** and **12a-l** were not shown activity; hence they have not incorporated.

***In vitro* anti-inflammatory activity [TNF-α and IL-6]**

*In vitro* anti-inflammatory activity based on TNF-α and IL-6 revealed that pyrazolyltriazole alcohol compounds showed better activity when compared to pyrazole alcohols (**Table 3**, **Fig. 1**). While analysis of activity at TNF-α and IL-6, compound **5f** denoted four-fold improved activity with IL-6 (**Table 3**). In case of pyrazolyltriazole alcohols, the compounds **8a-b**, **8e-f** and **8h** showed activity in TNF-α and IL-6. IL-6 based activity is much better to that of TNF-α, while standard compound showed similar activity profile with TNF-α and IL-6 (**Table 3**).

**Table 3.** Anti-inflammatory activity (TNF-α and IL-6) of the compounds **5a-h** and **8a-h**.

| Compound | TNF-α | | IL-6 | |
|---|---|---|---|---|
| | % Inhibition (10μM) | $IC_{50}$ (μM) | % Inhibition (10μM) | $IC_{50}$ (μM) |
| **5a** | 1.44 ± 0.60 | ND | 19.57 ± 0.23 | ND |
| **5b** | 3.32 ± 0.04 | ND | 24.11 ± 6.56 | ND |
| **5c** | 2.61 ± 0.92 | ND | 21.65 ± 1.48 | ND |
| **5d** | 0.74 ± 0.22 | ND | 20.87 ± 3.36 | ND |
| **5e** | ND | ND | 23.77 ± 6.95 | ND |
| **5f** | 22.95 ± 1.67 | 35.53 ± 2.34 | 68.47 ± 1.64 | 8.24 ± 1.48 |
| **5g** | 4.92 ± 0.84 | ND | 18.33± 5.23 | ND |
| **5h** | 8.35 ± 1.30 | ND | 46.36 ± 1.80 | ND |
| **8a** | 15.70 ± 1.10 | 35.74 ± 2.45 | 52.99 ± 4.22 | 8.12 ± 0.69 |
| **8b** | 19.24 ± 3.94 | 30.92 ± 1.50 | 76.94 ± 0.01 | 6.23 ± 0.23 |
| **8c** | 12.73 ± 4.68 | ND | 38.82 ± 0.86 | ND |
| **8d** | 14.75 ± 2.35 | ND | 42.04 ± 1.33 | ND |
| **8e** | 31.19 ± 3.51 | 21.39 ± 1.89 | 50.40 ± 3.52 | 8.70 ± 0.51 |
| **8f** | 40.88 ± 0.10 | 17.18 ± 1.01 | 46.73 ± 7.34 | 9.50 ± 1.03 |
| **8g** | 9.90 ± 2.78 | ND | 39.57 ± 9.06 | ND |
| **8h** | 41.73 ± 5.61 | 17.40 ± 0.92 | 87.00 ± 8.36 | 7.72 ± 0.82 |
| **Rolipram** | 59.13 ± 1.76 | 1.12 ± 0.03 | 53.53 ± 3.05 | 1.17 ± 0.49 |

ND: Not detected; results summarized in the table, for both % of cytokines inhibition presented as the mean ± SEM from three different experiments.

A)

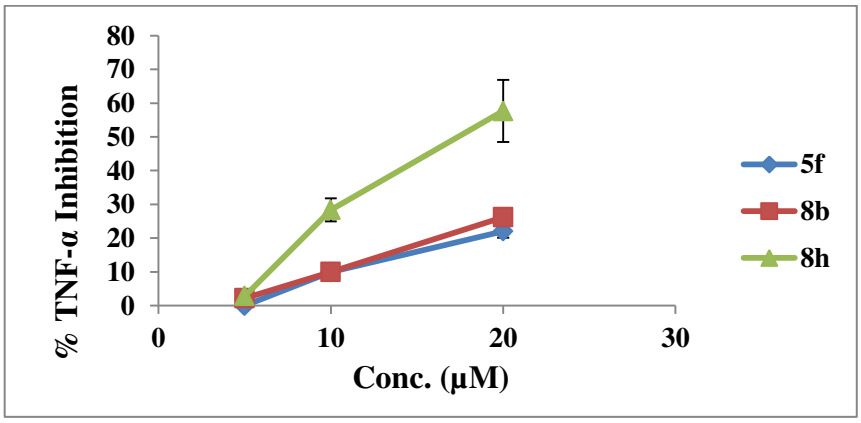


B)

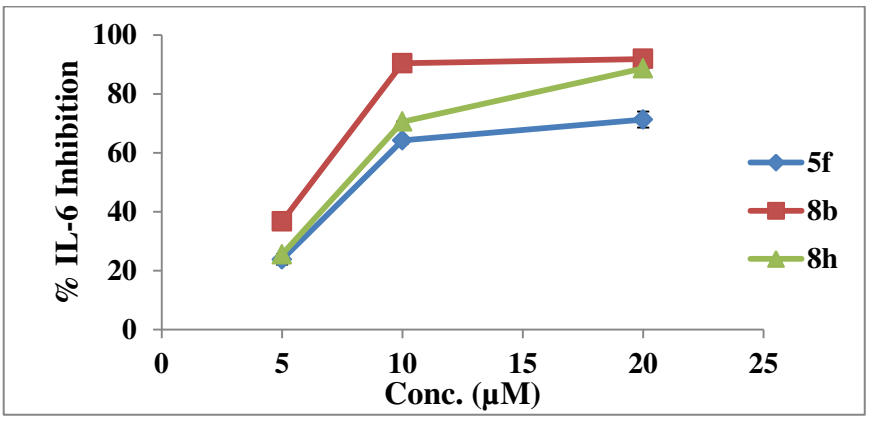


**Fig. 1**. The active compounds (**5f**, **8b** and **8h**) inhibit PMA/LPS-induced production of IL-6 and TNF-α in U937cells. U937 cells ($5 \times 10^4$ cells/ml) were pre-incubated for 30 minutes in the presence of the indicated concentrations of active compounds, and then they were treated with 100 ng/ml LPS for 24 hours (A, B). The concentration of TNF-α and IL-6 in the culture supernatants was measured using an ELISA assay. Data shown are typical of three independent experiments with similar results.

**Docking studies on TNF-α and IL-6**

Docking studies were performed to those compounds (**5f**, **8a-b**, **8e-f** and **8h**) showed the anti-inflammatory activity at *in vitro* analysis (**Table 4**) along with Rolipram as standard towards protein target 2AZ5 (TNF-α dimer) and 1ALU (IL-6). Among the tested compounds, compound **8b** showed the highest (-8.27, **Fig. 2**) binding energy while this value was lowest (-6.64) for **5f** against TNF-α, and Rolipram showed binding energy of -8.86 K.cal/mol. In case of IL-6, the compounds **8a** (-6.71) and **8f** (-5.55, **Fig. 3**) showed the highest and lowest binding energy values respectively, and the Rolipram showed -6.55 (**Table 4**).

**Table 4**. Dock score values for the compounds **5f, 8a-b, 8e-f** and **8h**.

| Compound | TNF-α | | IL-6 | |
|---|---|---|---|---|
| | Binding energy (XP glide score) (K.cal/mol) | Interactions | Binding energy (XP glide score) (K.cal/mol) | Interactions |
| **5f** | -6.64 | Leu120 | -5.57 | Lys66, Lys86 |
| **8a** | -7.51 | Tyr151 | -6.71 | Met67, Ser176 |
| **8b** | -8.27 | Tyr151, Gln61 | -6.44 | Met67, Ser176 |
| **8e** | -7.40 | Tyr151, Tyr151 | -5.79 | Lys86 |
| **8f** | -6.98 | Tyr151 | -5.55 | Lys86 |
| **8h** | -7.19 | Tyr151, Gln61 | -6.50 | Leu64 |
| **Rolipram** | -8.86 | Tyr151, Ser60 | -6.55 | Lys66, Ala68 |
| **Indomethacin** | -8.32 | Tyr151, Gly121 | -9.97 | Arg182, Arg179 |

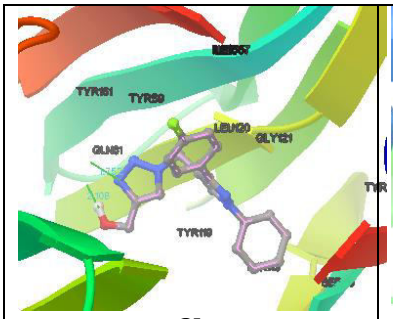


**8b**

**Fig. 2**. Docking pose of compounds **8b** with protein 2AZ5 (TNF-α dimer).

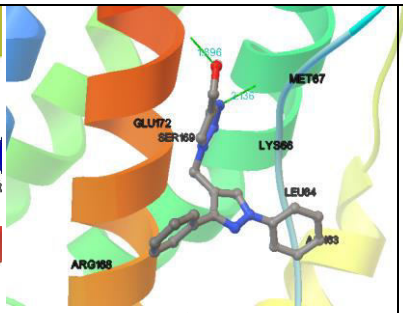


**8a**

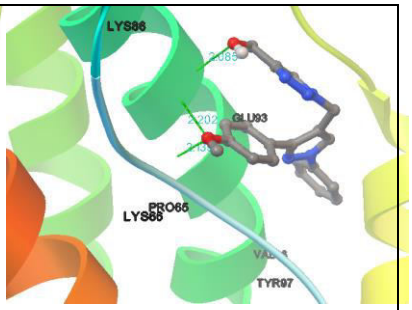


**8f**

**Fig. 3**. Docking pose of compounds **8a** and **8b** with protein 1ALU (IL-6).

***In vivo* anti-inflammatory activity by LPS challenged mouse model**

LPS has been implicated as an important pathogenic factor for the induction of sepsis, which is characterized by an inflammatory cytokine storm. Hence, *in vivo* anti-inflammatory activity of compounds **8b** and **8h** were evaluated on the basis of LPS induced cytokine expression in Balb/c mice (**Fig**. **4**). The challenge with LPS in mice showed significant (P<0.001) increase in TNF-α (**Fig**. **4A**) and IL-6 (**Fig**. **4B**) levels compared to the vehicle control group of animals. In the treatment groups, mice were pre-

treated with the test compounds **8b** and **8h** at a dose of 100 mg/kg for a period of 3 consecutive days followed by LPS challenge (10 mg/kg). Results indicated that the test compound **8h** had shown significant (P<0.01) inhibition in the TNF-α levels when compared to the LPS control animals, whereas the levels of IL-6 were not significantly (P<0.05) altered (**Fig**. **4**). Hence, compound **8h** may be considered as a good therapeutic agent to treat the inflammatory disease.

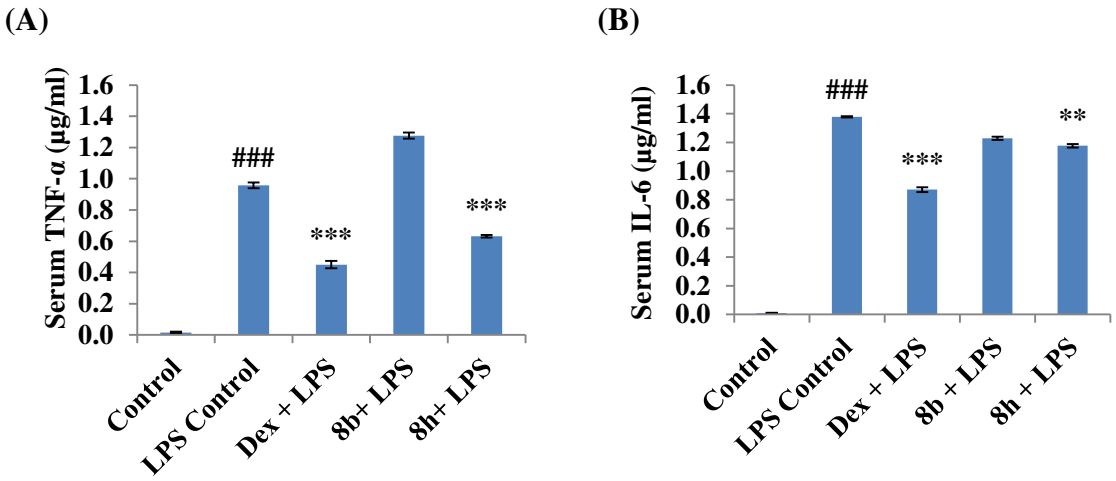


**Figure 4**. Effect of test compounds on LPS induced serum inflammatory cytokine secretions. ELISA of tumor necrosis factor-alpha (TNF-α) (A) and interleukin-6 (IL-6) (B). The results were expressed as mean ± S.E.M of 8 animals in each group. Control, vehicle control mice; LPS control, LPS control mice; LPS + Dex, LPS + Dexamethasone (2 mg/kg) treated mice; **8b** + LPS, LPS + **8b** (100 mg/kg) treated mice; **8h** + LPS, LPS + **8h** (100 mg/kg) treated mice. ### p<0.001 vs. Control; ** p<0.01 vs. LPS Control.

## PART-B, CHAPTER-II

**Synthesis and anti-cancer activity of pyridinylchalcones and chromanones.**

The present chapter describes the preparation of 2-chloronicotinaldehydes based i) chalcones **10a-q** and ii) chromanones **11a-q**. The prepared compounds were screened for their *in vitro* anti-cancer activity against four human cancer cell lines *viz*., cervical (HeLa), lung adenocarcinoma (A549), prostate (DU-145) and breast (MDA-MB-231). Further, the effective compound was confirmed the apoptotic effects in the cell cycle analysis.

**Preparation of 2-chloronicotinaldehydes** (**8a-e**).

2-Chloronicotinaldehydes **8a-e** were prepared from enamides by the Vilsmeier-Haack reaction. The enamides **4a-e** were prepared starting from commercially available aliphatic and aromatic aldehydes as depicted in scheme 1.

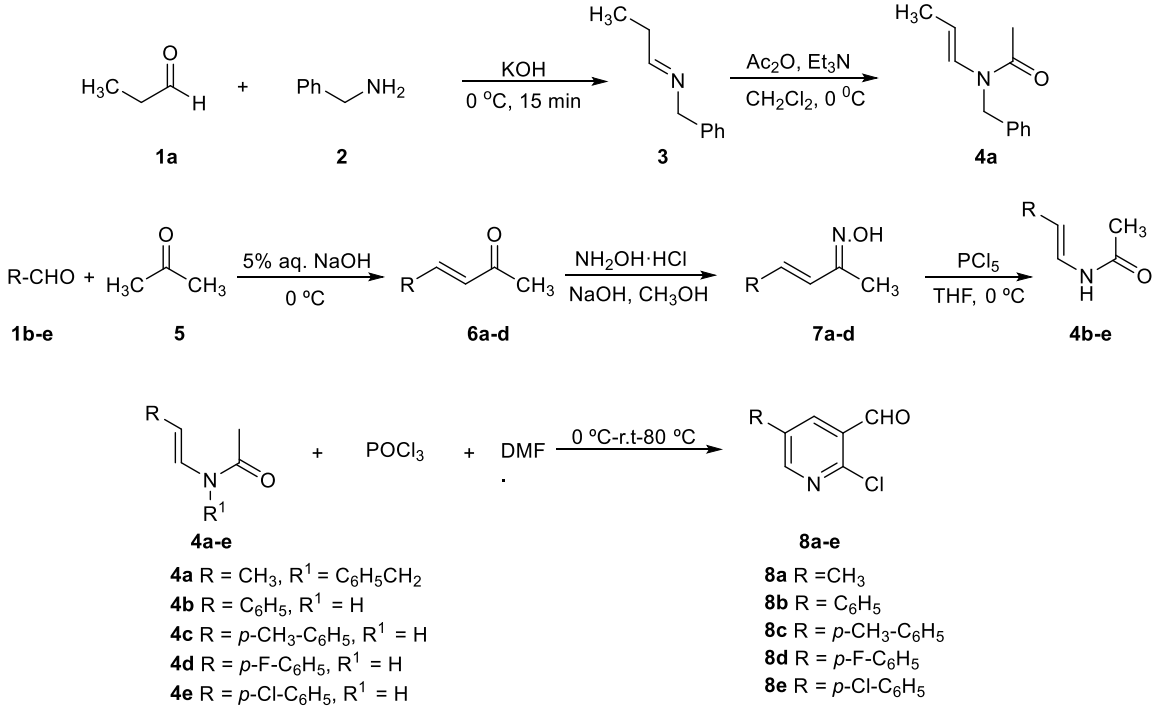


**Scheme 1**

**Preparation of pyridinylchalcones 10a-q and chromanones 11a-q**.

Claisen-Schmidt condensation of 2-chloronicotinaldehydes **8a-e** with 1-(2-hydroxyphenyl)ethanones **9a-e** in the presence of 40% aq. sodium hydroxide in ethyl alcohol at room temperature afforded the corresponding pyridinylchalcones **10a-q**. Cyclization of pyridinylchalcones **10a-q** in the presence of sodium acetate in ethyl alcohol under reflux conditions afforded the chromanones **11a-q** (**Scheme 2**).

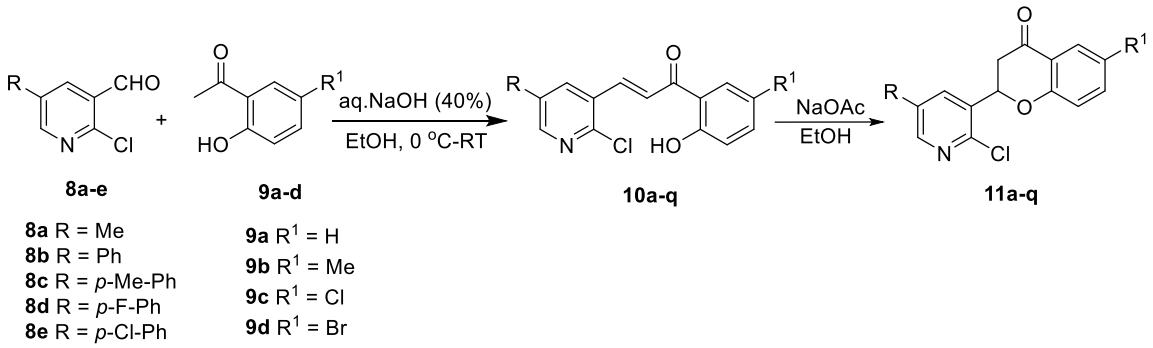


**Scheme 2**

## Biology

Pyridinylchalcones and chromanones were screened for their anti-cancer activity on four cancer cell lines namely; human epithetical cervical cancer (HeLa), lung adenocarcinoma (A549), prostate cancer (DU-145) and human breast cancer (MDA-MB-231) by MTT assay were presented in Table 1 & 2.

**Anti-cancer and structure-activity relationships of pyridinylchalcones** (**10a-q**).

The $IC_{50}$ values of compounds **10a-q** were depicted in Table 1. The compound having phenyl substitution on pyridinyl and methyl substitution on aromatic ring **10e** displayed better activity and $IC_{50}$ value of 5.9 µM in HeLa cell line and 12.5, 18.6 and 21.4 µM in A549, DU145 and MDA-MB-231 cell lines respectively.

**Table 1**. Anti-cancer activity of pyridinylchalcones **10a-q**.

| Compds | R | $R^1$ | Cytotoxicity ($IC_{50}$ μM) | | | |
|---|---|---|---|---|---|---|
| | | | HeLa | A549 | DU145 | MDA-MB- 231 |
| **10a** | Me | H | 13.4 ± 2.1 | 16.9 ± 2.7 | 26.2 ± 3.2 | 35.4 ± 3.5 |
| **10b** | Me | Cl | 51.4 ± 4.5 | 59.7 ± 3.8 | 86.7 ± 5.7 | 58.6 ± 4.5 |
| **10c** | Me | Br | 49.3 ± 2.9 | 65.5 ± 4.8 | 63.9 ± 3.1 | 47.1 ± 5.1 |
| **10d** | Ph | H | 25.5 ± 3.4 | 29.3 ± 3.1 | 45.0 ± 3.7 | 72.3 ± 5.9 |
| **10e** | Ph | Me | 5.9 ± 1.2 | 12.5 ± 2.1 | 18.6 ± 3.1 | 21.4 ± 3.1 |
| **10f** | Ph | Cl | 75.3 ± 6.2 | 44.3 ± 3.6 | 55 ± 3.9 | 49.8 ± 3.7 |
| **10g** | Ph | Br | 52.4 ± 4.9 | 58.5 ± 5.1 | 76.6 ± 6.1 | 74.7 ± 5.9 |
| **10h** | *p*-Me-Ph | H | 22.6 ± 2.1 | 28.1 ± 2.4 | 54.7 ± 3.3 | 81.1 ± 4.7 |
| **10i** | *p*-Me-Ph | Me | 15.6 ± 2.7 | 29.3 ± 2.5 | 31.8 ± 3.4 | 34 ± 4.5 |
| **10j** | *p*-Me-Ph | Cl | 64.3 ± 4.7 | 81.9 ± 5.1 | 91.6 ± 5.4 | 102.9 ± 7.7 |
| **10k** | *p*-Me-Ph | Br | 99.8 ± 10.5 | 104.6 ± 8.2 | 84.4 ± 6.2 | 127.5 ± 11.9 |
| **10l** | *p*-F-Ph | H | 57.7 ± 2.1 | 78.2 ± 4.7 | 62.6 ± 2.9 | 38.4 ± 3.7 |
| **10m** | *p*-F-Ph | Me | 46.3 ± 4.1 | 87.3 ± 5.2 | 78.6 ± 3.7 | 45.3 ± 2.9 |
| **10n** | *p*-F-Ph | Cl | 68.2 ± 3.6 | 90.8 ± 10.6 | 84.9 ± 5.9 | 67 ± 4.5 |
| **10o** | *p*-F-Ph | Br | 47.4 ± 2.7 | 70.7 ± 5.5 | 158.5 ± 7.1 | 59.7 ± 4.8 |
| **10p** | *p*-Cl-Ph | H | 51.9 ± 3.8 | 67.3 ± 4.6 | 141.6 ± 8.4 | 81.1 ± 6.6 |
| **10q** | *p*-Cl-Ph | Me | 42.0 ± 2.9 | 78.5 ± 4.3 | 237.9 ± 12.8 | 67.6 ± 3.6 |
| **Doxorubicin** | | | 2.25 ± 1.2 | 3.21 ± 0.8 | 3.74 ± 1.4 | 5.27 ± 1.8 |
| **Nocodazole** | | | 1.2 ± 0.84 | 1.0 ± 0.8 | 0.1 ± 0.08 | 1.0 ± 1.1 |

**Anti-cancer and structure-activity relationships of chromanones** (**11a-q**).

The $IC_{50}$ values of compounds **11a-q** were depicted in Table 2. Methyl substitution on pyridinyl and bromo group on aromatic ring **11c** displayed better activity and $IC_{50}$ value of 27.1 μM in HeLa cells.

Over all, the present study reveals that the chalcones displayed better activity when compared to chromanones. Compound **10e** is better among all the prepared compounds and chosen for caspase-3 activity and cell cycle analysis on HeLa cell line.

**Table 2**. Anti-cancer activity of pyridinylchromanones **11a-q**.

| | | | Cytotoxicity ($IC_{50}$ μM) | | | |
|---|---|---|---|---|---|---|
| | R | $R^1$ | HeLa | A549 | DU145 | MDA-MB- 231 |
| **11a** | Me | H | 78.6 ± 4.9 | 109.2 ± 8.9 | 140.7 ± 12.7 | 138.4 ± 13.6 |
| **11b** | Me | Cl | 78.08 ± 5.5 | 61 ± 4.6 | 68.2 ± 3.8 | 46.3 ± 2.9 |
| **11c** | Me | Br | 27.1 ± 3.2 | 46.1 ± 3.9 | 75.4 ± 6.3 | 57 ± 3.5 |
| **11d** | Ph | H | 58.1 ± 4.5 | 89.4 ± 9.2 | 74.8 ± 5.4 | 53.7 ± 4.6 |
| **11e** | Ph | Me | 59.7 ± 3.9 | 75.0 ± 5.5 | 98.6 ± 6.8 | 59.8 ± 4.9 |
| **11f** | Ph | Cl | 86.8 ± 7.5 | 139.6 ± 10.0 | 92.4 ± 6.4 | 48.7 ± 3.7 |
| **11g** | Ph | Br | 66.0 ± 6.9 | 129 ± 11.5 | 233.2 ± 14.5 | 112.4 ± 12.1 |
| **11h** | *p*-Me-Ph | H | 289 ± 15.3 | 196.7 ± 1.2 | 212.5 ± 12.5 | 145.9 ± 11.9 |
| **11i** | *p*-Me-Ph | Me | 93 ± 7.8 | 70.4 ± 5.6 | 83.1 ± 6.9 | 59.6 ± 3.8 |
| **11j** | *p*-Me-Ph | Cl | 149.1 ±11.6 | 65.7 ± 5.1 | 99.9 ± 8.3 | 71.7 ± 5.4 |
| **11k** | *p*-Me-Ph | Br | 91.7 ± 6.8 | 87.7 ± 4.1 | 89.6 ± 5.8 | 64.5 ± 3.4 |
| **11l** | *p*-F-Ph | H | 81.8 ± 5.1 | 74.3 ± 3.9 | 78.2 ± 3.5 | 57.5 ± 3.9 |
| **11m** | *p*-F-Ph | Me | 239 ± 18.5 | 95.5 ± 5.3 | 64.9 ± 3.9 | 45 ± 2.8 |
| **11m** | *p*-F-Ph | Cl | 261.6 ± 12 | 103.9 ± 10.5 | 70.7 ± 4.7 | 82.7 ± 4.5 |
| **11n** | *p*-F-Ph | Br | 89.6 ± 8.5 | 124.6 ± 11.2 | 71.8 ± 5.1 | 49.6 ± 3.7 |
| **11p** | *p*-Cl-Ph | H | 79.1 ± 6.3 | 35.5 ± 2.8 | 82.6 ± 6.4 | 71.4 ± 5.9 |
| **11q** | *p*-Cl-Ph | Me | 82.7 ± 5.7 | 89.6 ± 4.6 | 61.8 ± 3.9 | 67.7 ± 4.1 |
| **Doxorubicin** | | | 2.25 ± 1.2 | 3.21 ± 0.8 | 3.74 ± 1.4 | 5.27 ± 1.8 |
| **Nocodazole** | | | 1.2 ± 0.84 | 1.0 ± 0.8 | 0.1 ± 0.08 | 1.0 ± 1.1 |

**Activation of apoptosis by compound 10e**.

Caspases are the central regulators of both intrinsic and extrinsic pathways of apoptosis and caspase-3 is one of the effector caspase that is responsible for the majority of apoptotic processes through either intrinsic or extrinsic pathways. Results demonstrate that treatment of HeLa cells with compound **10e** resulted in a significant activation of caspase-3 by ~2 and 2.75-fold over controls at 7.5 and 10 μM respectively. Under similar experimental conditions, the proteasome inhibitor, bortezomib (1 μM), which was employed as a positive control induced nearly 3-fold increase in caspase-3 activity (**Fig. 1**).

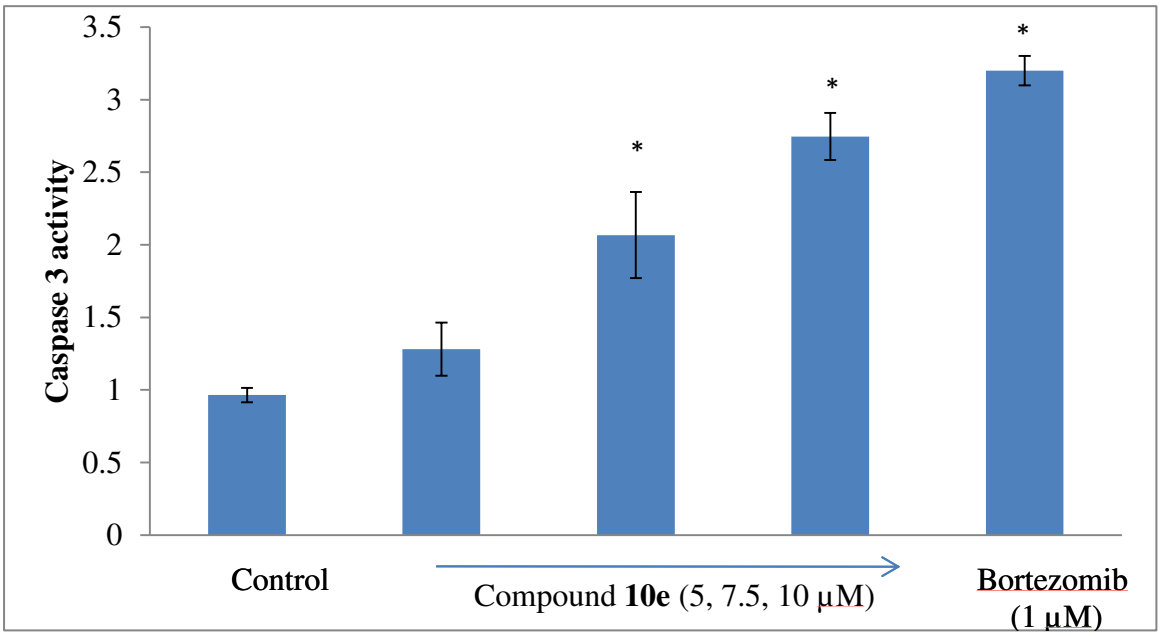


**Figure 1.** Determination of caspase-3 activity induced by compound **10e.**
Effect of compound **10e** on caspase-3 activity: HeLa cells were treated with compound **10e** (5-10 µM) and Bortezomib (1 µM) for 18 h. Following the termination of incubation, caspase-3 activity was measured using the tetra peptide substrate Ac-DEVD-AFC. Data represents mean ± SD of three different replicates and indicated as fold-increase with respect to control. * $p<0.01$ as compared to control

Further, cell cycle analysis of HeLa cells treated with **10e** exhibited a dose-dependent increase in the population of cells at sub-G1 phase from 5.47 % (control) to 25.93%, 31.13%, 31.45% at 5 µM, 7.5 µM and 10 µM concentration respectively (**Fig. 2**).

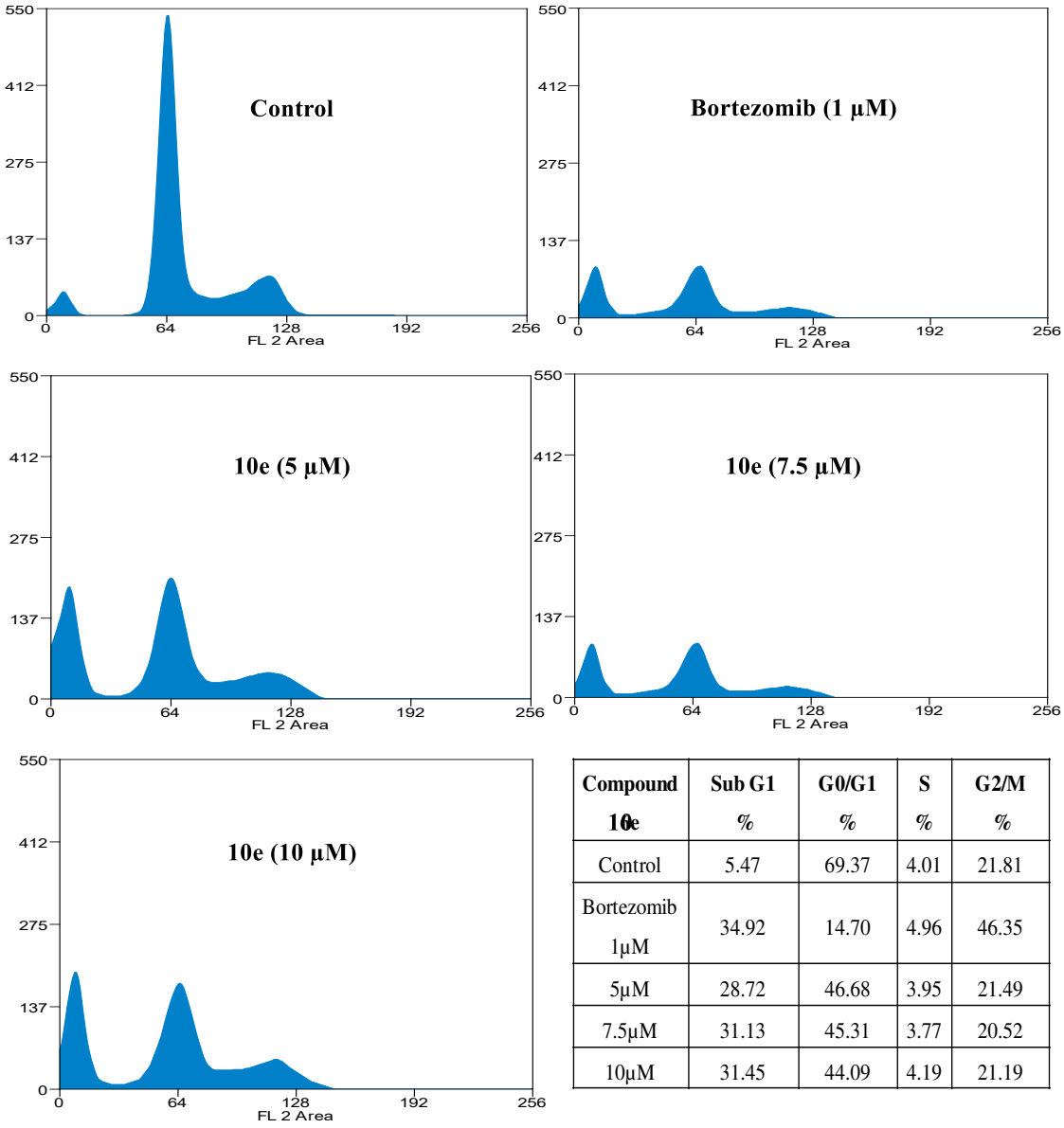


| Compound 10e | Sub G1 % | G0/G1 % | S % | G2/M % |
|---|---|---|---|---|
| Control | 5.47 | 69.37 | 4.01 | 21.81 |
| Bortezomib 1µM | 34.92 | 14.70 | 4.96 | 46.35 |
| 5µM | 28.72 | 46.68 | 3.95 | 21.49 |
| 7.5µM | 31.13 | 45.31 | 3.77 | 20.52 |
| 10µM | 31.45 | 44.09 | 4.19 | 21.19 |

**Figure 2.** Anti-mitotic effects of **10e** by FACS analysis.

The loss of mitochondrial potential as measured by JC-1 staining by **10e** (**Fig**. **3**) indicates that possibly the intrinsic pathway of apoptosis is responsible for **10e** induced anticancer effects.

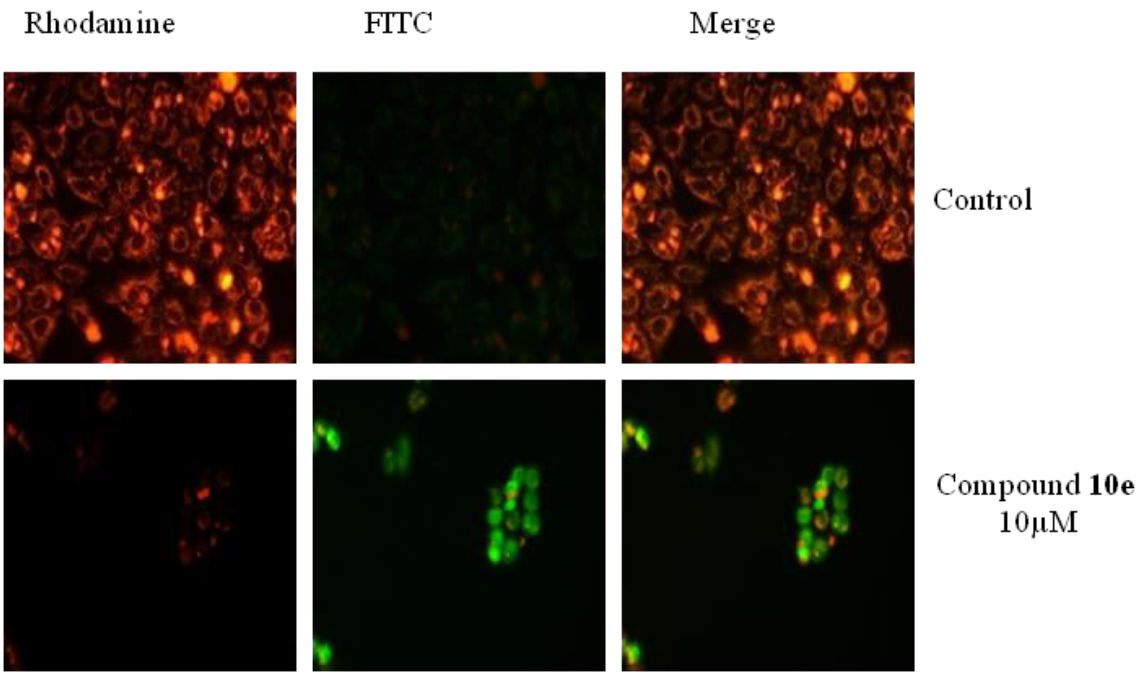


**Figure 3.** Effect of compound **10e** on microtubules and nuclear condensation.

Effect of compound **10e** on mitochondrial membrane potential: HeLa cells were treated with compound **10e** for 18 h. Following the termination of incubation, cells were treated with JC-1 dye as described in the "Materials and Methods" section. Fluorescence images of cells were captured using Olympus microscope (IX71) equipped with FITC and Rhodamine filter settings. Images are a representative of five different fields of view.

## CHAPTER-III, SECTION-A

**Synthesis of pyridinyl triazolylisonicotinohydrazides and their *anti-mycobacterial* activity.**

The present chapter describes the preparation of nicotinaldehyde based two series of compounds. I) 2-Chloropyridinyl triazolyisonicotinohydrazides (**7a-b**), II) pyridinylmorpholine and thio-morpholine triazolylisonicotinohydrazides (**13a-f**). The prepared compounds were screened for their *anti-mycobacterial* activity. Further, the effective *anti-tubercular* compounds were evaluated for their cytotoxicity.

**I) Preparation of 2-chloropyridinyl triazolylisonicotinohydrazides** (**7a-d**).

The $NaBH_4$ reduction of 2-chloronicotinaldehydes **1a-d** afforded the alcohols **2a-d**. The alcohols **2a-d** were converted to its corresponding azides **3a-d** in the presence of DPPA/DBU. Click reaction of azides **3a-d** with prop-2-yn-1-ol in the presence of $CuSO_4$/sodium ascorbate provided the triazolyl alcohols **4a-d**. Oxidation of triazolyl alcohols **4a-d** under IBX conditions provided the 2-chloropyridinyl triazolecarbaldehydes **5a-d**. Condensation of 2-chloropyridinyl triazolecarbaldehydes **5a-d** with isonicotinylhydrazine (INH, **6**) in ethanol, $H_2O$ medium at room temperature afforded the target compounds 2-chloropyridinyl triazolylisonicotinohydrazides **7a-d** (**Scheme 1**). The prepared 2-chloropyridinyl triazolylisonicotinohydrazides **7a-d** are unknown and well characterized by spectral data.

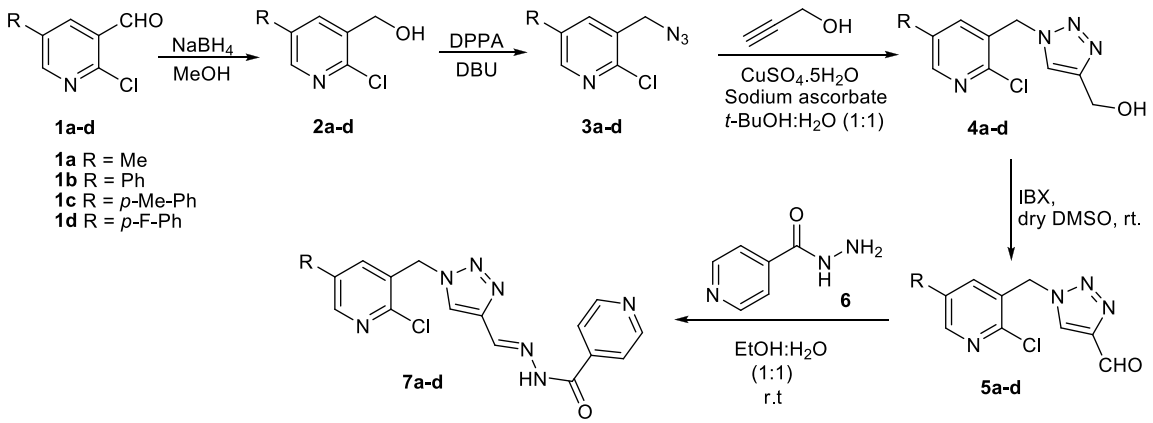


**Scheme 1**

Having achieved the preparation of 2-chloropyridinyl triazolylisonicotinohydrazides **7a-d**, we next prepared the morpholine, thio-morpholine containing 1*H*-1,2,3-triazolylisonicotinohydrazides **13a-f**.

**II) Preparation of pyridinylmorpholine and thio-morpholine triazolylisonicotinohydrazides** (**13a-f**).

2-Chloronicotinaldehydes **1a-c** were reacted with morpholine and thio-morpholine in the presence of $K_2CO_3$ in dry DMF at 110 °C furnished the nicotinaldehydes **8a-f**. Sequential reactions such as $NaBH_4$ reduction, azidation and click reaction of **8a-f** provided the triazolylalcohols **11a-f**. Oxidation of alcohols **11a-f** under IBX conditions furnished the 1*H*-1,2,3-triazole-4-carbaldehydes **12a-f**. Condensation of carbaldehydes **12a-f** with isonicotinylhydrazine (INH, **6**) in ethanol, $H_2O$ medium at room temperature afforded the target compounds pyridinylmorpholine and thio-morpholine triazolylisonicotinohydrazides **13a-f** (**Scheme 2**). The prepared pyridinylmorpholine and thio-morpholine triazolylisonicotinohydrazides **13a-f** are unknown and well characterized by spectral data.

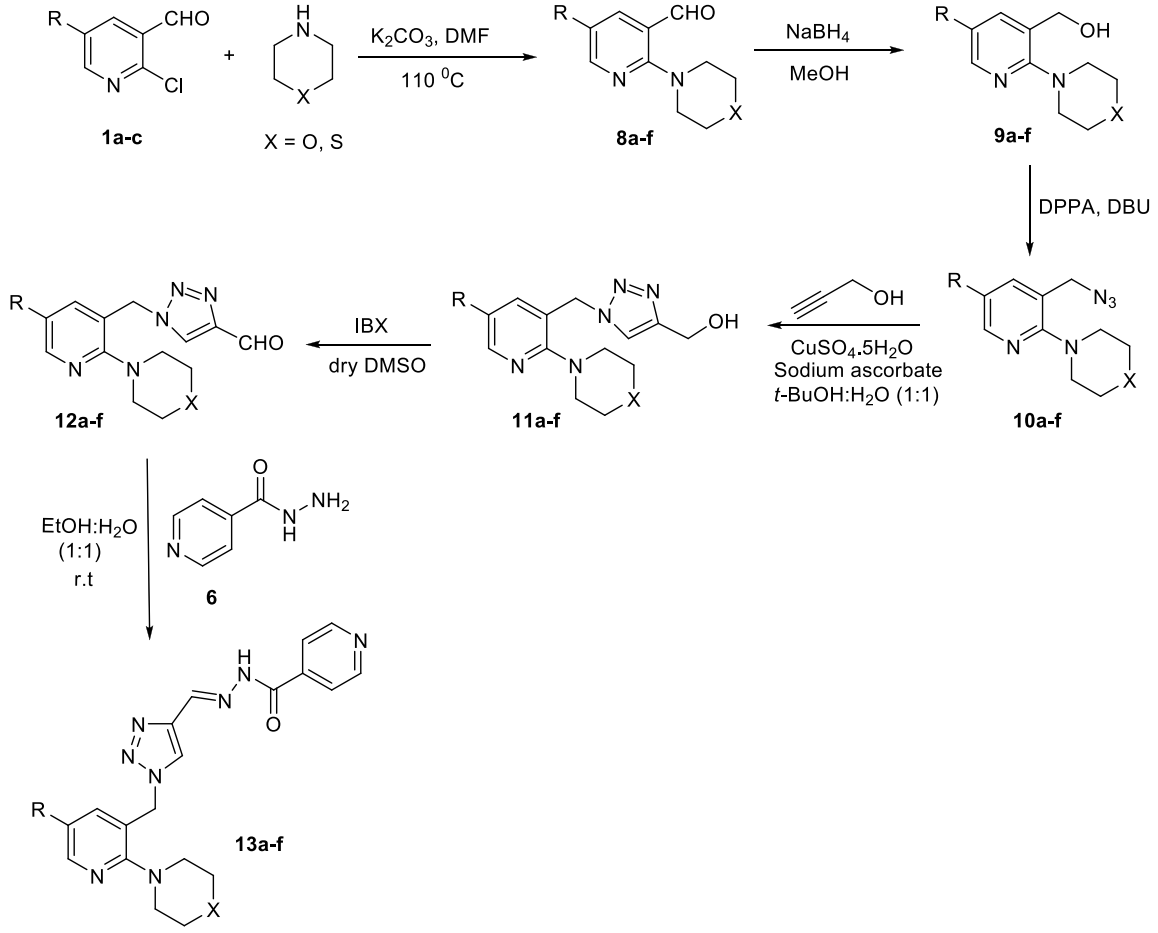


**Scheme 2**

Thus prepared compounds **7a-d** and **13a-f** were screened for their *in vitro anti-mycobacterial* activity against *M. tuberculosis* $H_{37}$RV strain (MTB) by microplate alamar blue assay (MABA). The MIC values of the prepared compounds along with standard drugs for comparison are presented in Table 1. The MIC's values for the prepared

compounds were ranging from 3.125-50 µg/mL and three compounds were inhibited MTB with less than 12.5 µg/mL. Methyl **7a** and phenyl **7b** substituted chloropyridyl compounds displayed significant *anti-mycobacterial* activity (12.5 µg/mL). Compound having methyl substitution at 5$^{th}$ position and thio-morpholine at 2$^{nd}$ position on pyridyl moiety **13b** displayed very good *anti-mycobacterial* activity (3.125 µg/mL).

Over all in the present series of compounds, the compound **13b** showed very good *anti-mycobacterial* activity and interesting molecule. The *in vitro anti-mycobacterial* activity of compounds **7a**, **7b** and **13b** were chosen to evaluate its cytotoxicity on RAW 264.7 cell lines. The % inhibition results were tabulated in Table 1. Compound **13b** inhibited 22.8%, **7a** inhibited 31.34%, **7b** inhibited 19.14% and indicated that these derivatives are not toxic.

**Table 1**. *Anti-mycobacterial* activity of compounds **7a-d**, **13a-f**, cytotoxicity of compounds **7a-b** and **13b.**

| Entry | Compound | R | X | MIC (µg/mL) | MIC (µM) | RAW 264.7 cells (% inhibition) |
|---|---|---|---|---|---|---|
| 1 | **7a** | Me | -- | 12.5 | 35.21 | 31.34 |
| 2 | **7b** | Ph | -- | 12.5 | 29.97 | 19.14 |
| 3 | **7c** | *p*-$MeC_6H_4$ | -- | 25 | 58.00 | NT |
| 4 | **7d** | *p*-$FC_6H_4$ | -- | 25 | 57.47 | NT |
| 5 | **13a** | Me | O | 50 | 98.88 | NT |
| 6 | **13b** | Me | S | 3.125 | 7.44 | 22.86 |
| 7 | **13c** | Ph | O | 50 | 108.22 | NT |
| 8 | **13d** | Ph | S | 25 | 51.65 | NT |
| 9 | **13e** | *p*-$MeC_6H_4$ | O | 50 | 103.73 | NT |
| 10 | **13f** | *p*-$MeC_6H_4$ | S | 25 | 48.63 | NT |
| | Isoniazide | | | 0.4 | | |
| | Rifampicine | | | 0.02 | | |

NT – not tested

## CHAPTER-III, SECTION-B

**Synthesis and biological activities of nicotinaldehyde based azlactones.**

The present chapter describes the preparation of nicotinaldehyde based four series of compounds. I) Pyridinylazlactones (**3a-g**), II) pyridinyl morpholine and thio-morpholine azlactones (**6a-f**), III) pyridinyltriazolyl azlactones (**11a-d**) and IV) pyridinyl morpholine and thio-morpholine triazolylazlactones (**16a-d**). The prepared compounds **3a-g**, **6a-f**, **11a-d** and **16a-d** were evaluated for their DPPH and ABTS free radical scavenging, α-glucosidase and anti-cancer activities.

**I. Preparation of pyridinylazlactones** (**3a-f**).

The condensation reaction of nicotinaldehydes **1a-f** with hippuric acid **2** in the presence of sodium acetate and acetic anhydride provided the azlactones **3a-f** (**Scheme 1**).

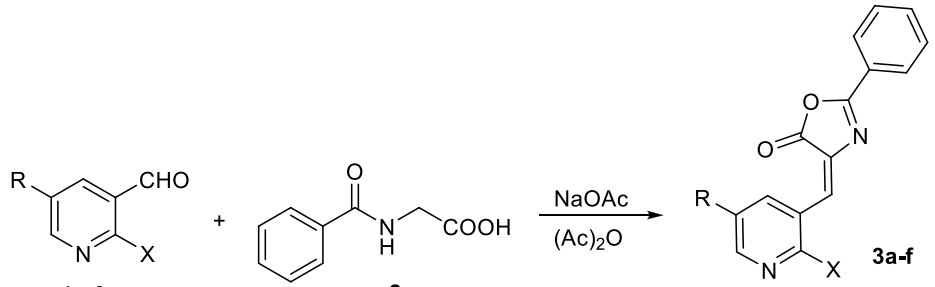


**3a** R = H, X = H
**3b** R = H, X = Cl
**3c** R = $CH_3$, X = Cl
**3d** R = Ph, X = Cl
**3e** R = *p*-Me-Ph, X = Cl
**3f** R = *p*-F-Ph, X = Cl

**Scheme 1**

Scheme 2 describes the preparation of 4-pyridinylazlactone **3g** by the condensation of 4-pyridinecarbaldehyde with hippuric acid **2** in the presence of sodium acetate and acetic anhydride.

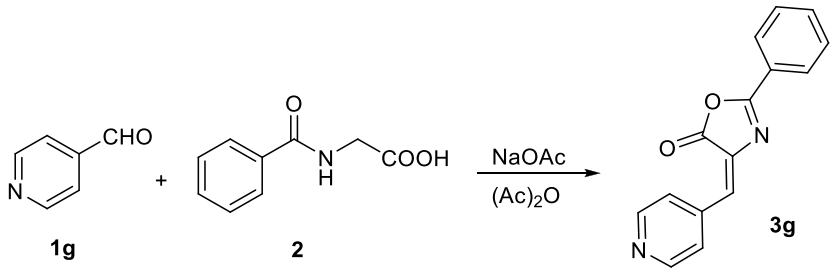


**Scheme 2**

**II. Preparation of pyridinylmorpholine and thio-morpholine azlactones** (**6a-f**).

2-Chloronicotinaldehydes **1c-e** were reacted with morpholine **4a** and thio-morpholine **4b** in the presence of $K_2CO_3$ in dry DMF at 110 °C and furnished the corresponding compounds **5a-f**. Condensation of **5a-f** with hippuric acid **2** in the presence of sodium acetate and acetic anhydride provided the azlactones **6a-f** (**Scheme 3**).

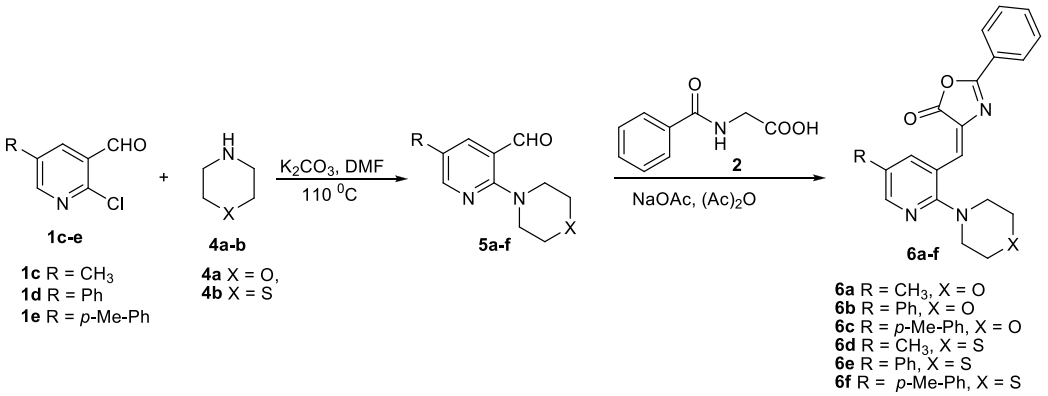


**Scheme 3**

**III. Preparation of pyridinyltriazolyl azlactones** (**11a-d**).

$NaBH_4$ reduction of 2-chloronicotinaldehydes **1c-f** in methanol at 0 °C furnished the alcohols **7a-d**. Azidation of alcohols **7a-d** with diphenylphosphoryl azide (DPPA) in the presence of DBU at room temperature afforded the azides **8a-d**. Cycloaddition of azides **8a-d** with propargyl alcohol in the presence of $CuSO_4$/sodium ascorbate at room temperature provided the triazolylalcohols **9a-d**. Oxidation of alcohols **9a-d** under IBX conditions furnished the 1*H*-1,2,3-triazole-4-carboxaldehydes **10a-d**. Condensation of **10a-d** with hippuric acid **2** in the presence of sodium acetate and acetic anhydride provided the azlactones **11a-d** (**Scheme 4**).

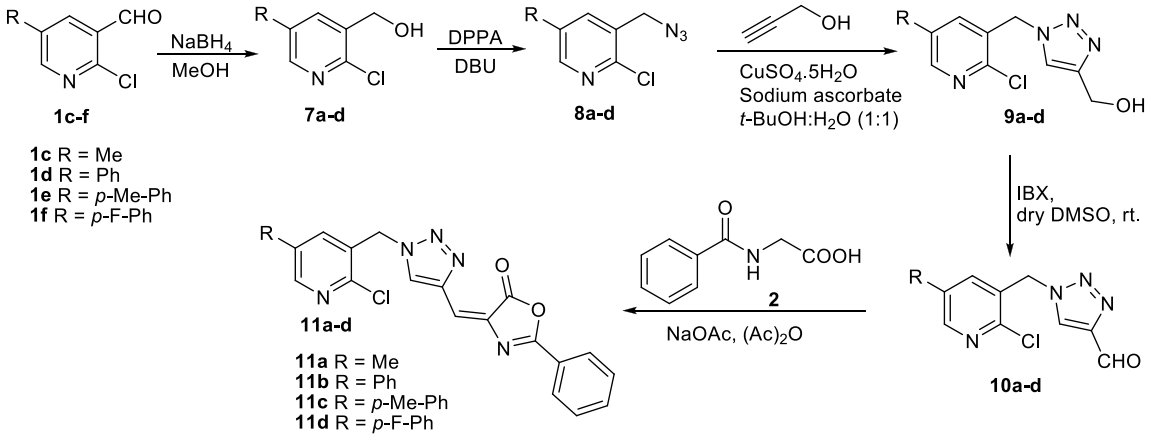


**Scheme 4**

**IV) Preparation of pyridinylmorpholine and thio-morpholine triazolylazlactones (16a-d).**

2-Chloronicotinaldehydes **1d-e** were reacted with morpholine **4a** and thio-morpholine **4b** in the presence of $K_2CO_3$ in dry DMF at 110 °C and furnished the compounds **5b-c** and **5e-f**. Sequential reactions such as reduction, azidation and click reaction of **5b-c** and **5e-f** provided the triazolylalcohols **14a-d**. Oxidation of alcohols **14a-d** under IBX conditions furnished the pyridinyl triazolecarbaldehydes **15a-d**. Condensation of **15a-d** with hippuric acid **2** in the presence of sodium acetate and acetic anhydride provided the azlactones **16a-d** (**Scheme 5**). Thus prepared azlactones **3a-g, 6a-f, 11a-d, 16a-d** are unknown compounds and well characterized by IR, $^1$H NMR, $^{13}$C NMR and mass spectroscopy.

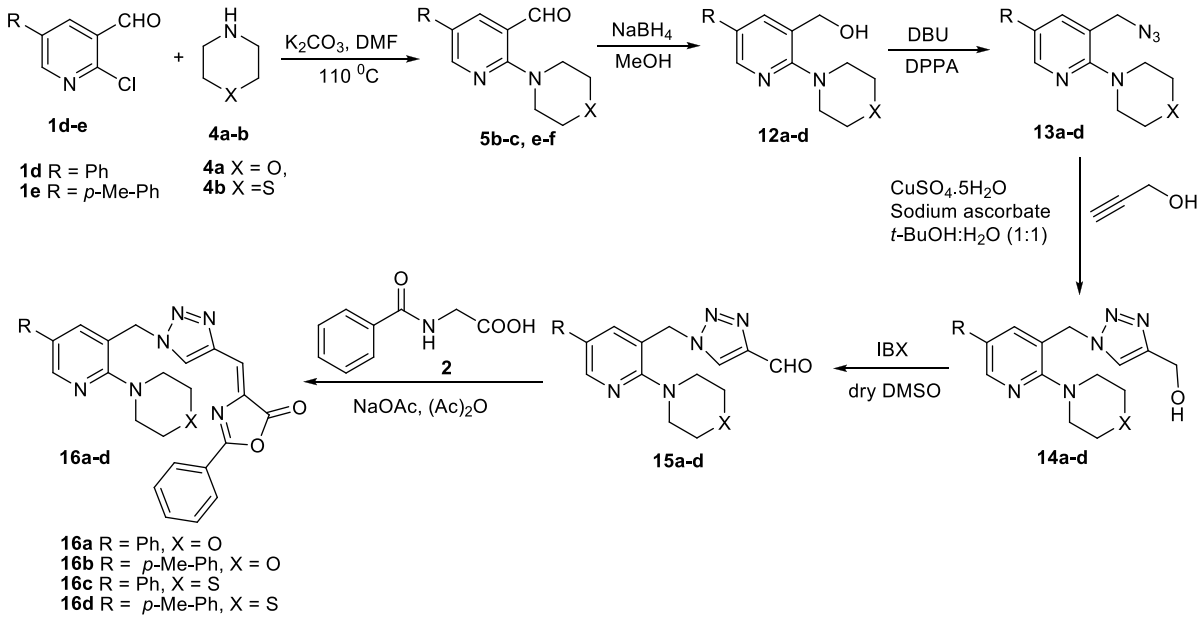


**Scheme 5**

The prepared azlactones **3a-g, 6a-f, 11a-d** and **16a-d** were evaluated for their DPPH, $ABTS^{+\cdot}$ free radical scavenging and α-glucosidase inhibitory activities. These compounds were also tested for their anti-cancer activity on three cancer cell lines namely lung adenocarcinoma (A549), human breast cancer (MCF7) and human epithelial cervical cancer (HeLa) by MTT assay and compared with the standard drug doxorubicin.

**DPPH and $ABTS^{+\cdot}$ free radical scavenging activities of azlactones**

The DPPH and $ABTS^{+\cdot}$ radical scavenging activity profiles of azlactones **3a-g**, **6a-f**, **11a-d**, and **16a-d** are presented in Table 1. Pyridylazlactones **3a-g** and 2-morpholine and thio-morpholine pyridylazlactones **6a-f** could not scavenge DPPH and $ABTS^{+\cdot}$

radicals. The pyridyltriazolyl azlactone **11b** displayed the DPPH ($SC_{50}$, 46.70 µg/mL) and $ABTS^{+\cdot}$ ($SC_{50,}$ 39.31 µg/mL) scavenging activity.

**α-Glucosidase inhibitory activity of azlactones**

The intestinal α-glucosidase enzyme plays an important role in digestion of dietary carbohydrate. Inhibition of the enzyme has become an important target in mitigating excursion in postprandial hyperglycemia (PPHG) in diabetic individual. The percentage inhibition and $IC_{50}$ of α-glucosidase inhibitory activity values for the azlactones **3a-g, 6a-f, 11a-d** and **16a-d** are presented in Table 1. Among the screened compounds the 4-pyridinylazlactone **3g** ($IC_{50,}$ 15.05 µg/mL) displayed potent α-glucosidase inhibitory activity.

**Anti-cancer activity of azlactones**

The $IC_{50}$ values of azlactones **3a-g**, **6a-f**, **11a-d** and **16a-d** along with the standard drug doxorubicin are presented in Table 2. *p*-Methylphenyl and *p*-fluorophenyl triazolylpyridinyl azlactones (**11c-d**) and *p*-methylphenyl thio-morpholine triazolylpyridinyl azlactone (**16d**) displayed anti-cancer activity on all the tested cell lines. However, *p*-methylphenyl morpholine (**16b**) and phenyl thio-morpholine (**16c**) triazolylpyridinyl azlactones displayed selectively on MCF7 and HeLa cell lines.

**Table 1.** DPPH, $ABTS^{+\cdot}$ free radical scavenging and α-glucosidase inhibitory activities of azlactones **3a-g**, **6a-f**, **11a-d** and **16a-d**.

| Compound | DPPH % Inhibition at 25 µg/mL ($SC_{50}$ µg/mL) | ABTS % Inhibition at 20 µg/mL ($SC_{50}$ µg/mL) | AGI % Inhibition at 20 µg/mL ($IC_{50}$ µg/mL) |
|---|---|---|---|
| **3a** | 25.81 | 37.39 | ND |
| **3b** | 42.32 | 57.38 | ND |
| **3c** | ND | ND | ND |
| **3d** | 0.63 | ND | ND |
| **3e** | 2.09 | ND | ND |
| **3f** | ND | ND | 39.00 |
| **3g** | 9.20 | 9.29 | 92.61 (15.05) |
| **6a** | 9.53 | 10.66 | 61.55 (37.05) |
| **6b** | 1.71 | ND | 78.93 (20.22) |
| **6c** | 5.50 | 11.35 | ND |
| **6d** | ND | ND | 59.33 |
| **6e** | 7.46 | 8.73 | 42.69 |
| **6f** | ND | ND | ND |
| **11a** | ND | ND | ND |
| **11b** | 55.62 (46.70) | 67.01 (39.31) | ND |
| **11c** | 0.48 | ND | ND |
| **11d** | ND | ND | 30.13 |
| **16a** | 16.91 | 23.24 | 49.35 |
| **16b** | 25.26 | 38.12 | 3.88 |
| **16c** | 16.86 | 24.01 | ND |
| **16d** | 28.93 | 40.09 | ND |
| Ascorbic acid | 72.90 (28.08) | ---- | ---- |
| Trolox | ---- | 80.20 (18.42) | ---- |
| Acarbose | ---- | ---- | 98.99 (12.57) |

**Table 2**. Anti-cancer activity of azlactones **3a-g**, **6a-f**, **11a-d** and **16a-d.**

| Compound[a,b] | MCF7 | A549 | HeLa |
|---|---|---|---|
| **3a** | ND | ND | ND |
| **3b** | ND | ND | ND |
| **3c** | 23.12 ± 0.19 | 50.05 ± 0.15 | 28.45 ± 0.16 |
| **3d** | 23.94 ± 0.09 | 32.90 ± 0.10 | 27.34 ± 0.08 |
| **3e** | 20.85 ± 0.26 | 27 ± 0.09 | 20.46 ± 0.08 |
| **3f** | 25 ± 0.33 | 37.84 ± 0.09 | 20.39 ± 0.10 |
| **3g** | ND | ND | ND |
| **6a** | 21.60 ± 0.05 | 32.16 ± 0.09 | 27.31 ± 0.07 |
| **6b** | 26.07 ± 0.12 | 31.55 ± 0.18 | 19.48 ± 0.17 |
| **6c** | 25.59 ± 0.21 | 28.08 ± 0.11 | 22.30 ± 0.05 |
| **6d** | 21.55 ± 0.08 | 33.88 ± 0.10 | 33.36 ± 0.07 |
| **6e** | 26.54 ± 0.13 | 27.53 ± 0.10 | 24.29 ± 0.12 |
| **6f** | 25.83 ± 0.33 | 28.91 ± 0.09 | 19.43 ± 0.07 |
| **11a** | ND | ND | ND |
| **11b** | 20.31 ± 0.14 | 36.83 ± 0.08 | 17.74 ± 0.09 |
| **11c** | 17.23 ± 0.11 | 18.70 ± 0.03 | 17.73 ± 0.06 |
| **11d** | 14.66 ± 0.10 | 16.8 ± 0.08 | 15.53 ± 0.04 |
| **16a** | 22.29 ± 0.12 | 31.61 ± 0.11 | 24.55 ± 0.09 |
| **16b** | 18.21 ± 0.20 | 23.75 ± 0.04 | 16.59 ± 0.04 |
| **16c** | 18.58 ± 0.04 | 24.01 ± 0.02 | 17.63 ± 0.04 |
| **16d** | 14.08 ± 0.16 | 17.84 ± 0.03 | 14.84 ± 0.01 |
| Doxorubicin | 4.05 ±1.2 | 2.89 ±1.1 | 3.03 ± 1.1 |

[a)] Cell lines were treated with different concentrations of compounds for 48 h. Cell viability was measured employing MTT assay.
[b)] $IC_{50}$ (μM) values are indicated as the mean ± SD of three independent experiments. ND-Not detected

## PART-C, CHAPTER-IV

**Synthesis of benzimidazoles, pyrazolones and pyrazoles.**

The present chapter describes the preparation of three series of compounds such as I) chloromethyl benzimidazoles (**3a-f**), II) chloromethyl pyrazolones (**5a-b**) and chloromethyl alkoxy pyrazoles (**6a-e**), III) alkoxymethyl pyrazolones (**7a-o**) and alkoxymethyl pyrazoles (**8a-j**). Chloromethyl benzimidazoles (**3a-f**) has been prepared by the condensation of *o*-phenylenediamines with ethyl 4-chloro-3-oxobutanoate. Chloromethyl pyrazolones (**5a-b**) and chloromethyl alkoxy pyrazoles (**6a-e**) have been prepared by the condensation of phenylhydrazine hydrochlorides with ethyl 4-chloro-3-oxobutanoate. Phenylhydrazine hydrochlorides with ethyl 4-chloro-3-oxobutanoate in polar protic solvents under went *in situ* nucleophilic substitution reaction and provided the corresponding alkoxymethyl pyrazolones (**7a-o**) and alkoxymethyl pyrazoles (**8a-j**).

**I. Preparation of chloromethyl benzimidazoles** (**3a-f**).

In a model reaction, ethyl 4-chloro-3-oxobutanoate **2** (1 mmol) was added to a stirred solution of *o*-phenylenediamine **1a** (1 mmol) in $CH_3CN$ (2 mL) at room temperature (38 h). This furnished a pale yellow product (**Scheme 1**) and based on spectral data the compound identified as 2-(chloromethyl)-1*H*-benzo[*d*]imidazole **3a**.

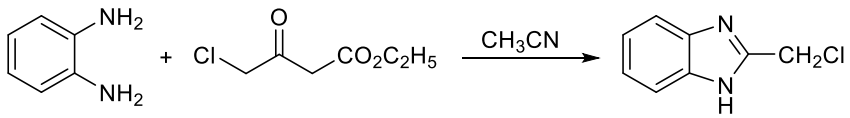


**1a** **2** **3a**

**Scheme 1**

The present reaction has been investigated with various solvents, catalysts and the results were summarized in Table 1. The yield of **3a** was improved to 82% in the presence of $SnCl_2$ in $C_2H_5OH$ under reflux conditions.

**Table 1.** Preparation of 2-(chloromethyl)-1*H*-benzo[*d*]imidazole **3a**[a]

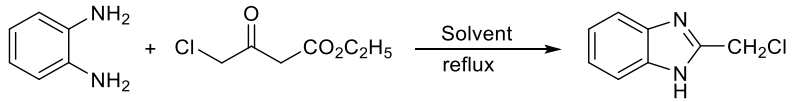


**1a** **2** **3a**

| Entry | Catalyst | Solvent | Reaction Time, (h) | Yield[d] (%) **3** |
|---|---|---|---|---|
| 1 | -- | $CH_3CN$ [b] | 38 | 40 |
| 2 | -- | $CH_3CN$[c] | 20 | 40 |
| 3 | -- | $CH_3OH$ [b] | 18 | 48 |
| 4 | -- | $CH_3OH$ [c] | 12 | 62 |
| 5 | -- | $C_2H_5OH$ [b] | 32 | 56 |
| 6 | -- | $C_2H_5OH$ [c] | 12 | 68 |
| 7 | -- | THF [c] | 24 | 52 |
| 8 | -- | $CH_2Cl_2$ [c] | 18 | 63 |
| 9 | AcOH | $C_2H_5OH$ [c] | 10 | 70 |
| 10 | *p*-TsOH | $C_2H_5OH$ [c] | 12 | 72 |
| 11 | $AlCl_3$ | $C_2H_5OH$ [c] | 8 | 65 |
| 12 | CuI | $C_2H_5OH$ [c] | 8 | 70 |
| 13 | $CuCl_2$ | $C_2H_5OH$ [c] | 10 | 65 |
| 14 | $Cu(OAc)_2$ | $C_2H_5OH$ [c] | 9 | 60 |
| **15** | **$SnCl_2$** | **$C_2H_5OH$ [c]** | **6** | **82** |
| 16 | $La(OTf)_3$ | $C_2H_5OH$ [c] | 10 | 66 |
| 17 | $Sc(OTf)_3$ | $C_2H_5OH$ [c] | 8 | 69 |
| 18 | $Bi(OTf)_3$ | $C_2H_5OH$ [c] | 8 | 72 |

[a] Conditions: *o*-Phenylenediamine (1 mmol), ethyl 4-chloro-3-oxobutanoate (1 mmol), catalyst (0.1 mmol), [b] rt, [c] reflux, [d] Yields of isolated products.

In order to evaluate the scope of this methodology, substituted *o*-phenylenediamines were reacted with **2** having electron withdrawing and donating substituents and this provided a series of 2-(chloromethyl)-1*H*-benzo[*d*]imidazoles **3b**-**f** in good yields (**Table 2**).

**Table 2.** Preparation of 2-(chloromethyl)-1*H*-benzo[*d*]imidazoles **3a-f**

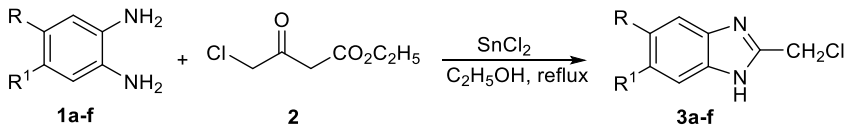


| Entry | Reactant **1** | R | $R^1$ | Reaction Time, [h] | Product **3** | Yield[a] (%) |
|---|---|---|---|---|---|---|
| 1 | **1a** | H | H | 6 | **3a** | 82 |
| 2 | **1b** | $NO_2$ | H | 5 | **3b** | 75 |
| 3 | **1c** | Cl | H | 6 | **3c** | 72 |
| 4 | **1d** | COPh | H | 8 | **3d** | 60 |
| 5 | **1e** | $CH_3$ | H | 6 | **3e** | 65 |
| 6 | **1f** | $CH_3$ | $CH_3$ | 8 | **3f** | 62 |

[a] Yields of isolated products.

Having succeeded in the preparation of 2-chloromethyl-1*H*-benzimidazoles, next the reaction has been studied with phenylhydrazine hydrochlorides **4a-e** and ethyl 4-chloro-3-oxobutanoate **2** (**Scheme 2**). In a model reaction, **2** (1 mmol) was added to a stirred solution of phenylhydrazine hydrochloride **4a** (1 mmol) in $CH_3CN$ (2 mL) at room temperature. This reaction furnished two compounds, based on spectral data the compound identified as 3-(chloromethyl)-1-phenyl-1*H*-pyrazol-5(4*H*)-one (**5a,** 30%) and 3-(chloromethyl)-5-ethoxy-1-phenyl-1*H*-pyrazole (**6a**, 15%). These compounds were well characterized by spectral data.

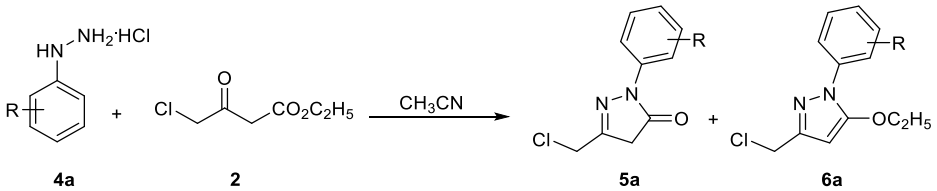


**Scheme 2**

To study the product selectivity, various catalysts and solvents were investigated and summarized in Table 3. Among them, $Bi(OTf)_3$ in THF under reflux condition provided **5a** in 62 % yield and **6a** in 5 % yield (entry 15).

**Table 3.** Preparation of 1*H*-pyrazolone **5** and pyrazole **6**[a]

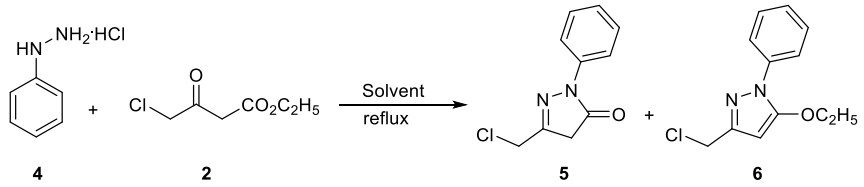


4 2 5 6

| Entry | Catalyst | Solvent | Reaction time, (h) | Yield[c] (%) **5** | Yield[c] (%) **6** |
|---|---|---|---|---|---|
| 1 | -- | $CH_2Cl_2$ [b] | 24 | -- | -- |
| 2 | -- | $CH_2Cl_2$ | 24 | -- | -- |
| 3 | -- | Toluene | 48 | -- | -- |
| 4 | -- | $CH_3CN$ | 14 | 30 | 15 |
| 5 | -- | THF | 18 | 40 | 18 |
| 6 | AcOH | THF | 16 | 42 | 15 |
| 7 | *p*-TsOH | THF | 18 | 35 | 14 |
| 8 | $FeCl_3$ | THF | 20 | 28 | 10 |
| 9 | $AlCl_3$ | THF | 24 | 32 | 13 |
| 10 | $Cu(OAc)_2$ | THF | 20 | 30 | 14 |
| 11 | $CuCl_2$ | THF | 18 | 20 | 08 |
| 12 | $SnCl_2$ | THF | 20 | 25 | 11 |
| 13 | $La(OTf)_3$ | THF | 18 | 46 | 14 |
| 14 | $Sc(OTf)_3$ | THF | 18 | 50 | 11 |
| **15** | **$Bi(OTf)_3$** | **THF** | **12** | **62** | **05** |
| 16 | $Bi(OTf)_3$ | $CH_3CN$ | 12 | 56 | 08 |

[a]Conditions: Phenylhydrazine hydrochloride (1 mmol), ethyl 4-chloro-3-oxobutanoate (1 mmol), catalyst (0.1 mmol), under reflux. [b] rt. [c] Yields of isolated products.

In order to evaluate the efficiency of this methodology, phenylhydrazine hydrochlorides having electron withdrawing and donating substituents **4a-e** were reacted with **2** provided the corresponding pyrazolones **5a-b** and pyrazoles **6a-e** (**Table 4**)

**Table 4**. Preparation of 1*H*-pyrazolones **5a-b** and pyrazoles **6a-e**[a]

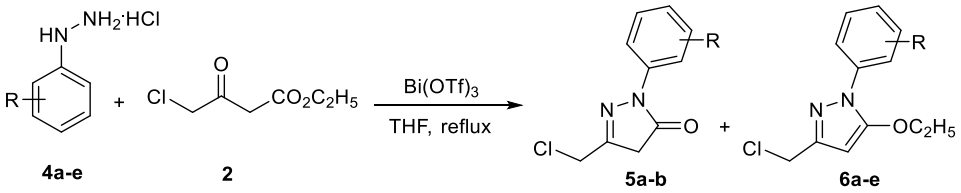


4a-e 2 5a-b 6a-e

| Entry | Reactant **4** | R | Reaction Time, (h) | Product **5** | Yield[b] (%) | Product **6** | Yield[b] (%) |
|---|---|---|---|---|---|---|---|
| 1 | **4a** | H | 12 | **5a** | 62 | **6a** | 05 |
| 2 | **4b** | *m*-$NO_2$ | 18 | **5b** | 52 | **6b** | 10 |
| 3 | **4c** | *p*-F | 20 | -- | -- | **6c** | 18 |
| 4 | **4d** | *p*-$CH_3$ | 24 | -- | -- | **6d** | 20 |
| 5 | **4e** | *p*-$NO_2$ | 32 | -- | -- | **6e** | 22 |

[a] Conditions: Phenylhydrazine hydrochloride (1 mmol), ethyl 4-chloro-3-oxobutanoate (1 mmol), $Bi(OTf)_3$ (0.1 mmol), under reflux. [b] Yields of isolated products.

Further, the condensation reaction has been carried out with **4a** (1 mmol) and **2** (1 mmol) in the presence of $Bi(OTf)_3$ (0.1 mmol) in $CH_3OH$ under reflux conditions. This reaction furnished two pale yellow products and identified as 3-(methoxymethyl)-1-phenyl-1*H*-pyrazol-5(4*H*)-one **7a** (52% yield) and 5-ethoxy-3-(methoxymethyl)-1-phenyl-1*H*-pyrazole **8a** (15%, **Scheme 3**).

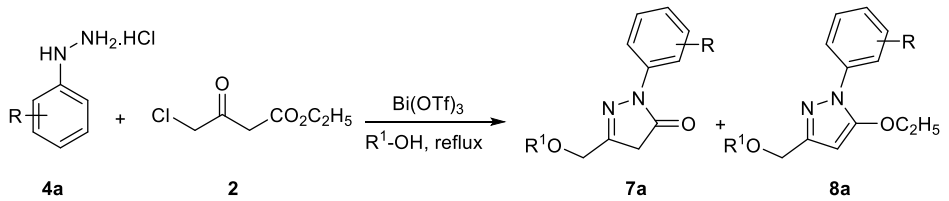


4a 2 7a 8a

**Scheme 3**

This reaction provided an interesting result that the nucleophilic substitution has been occurred *in situ*. The reaction prompted us to study in detail with various alcoholic solvents and the results were summarized in Table 5. Under similar conditions, the reaction of **4a** with **2** in $C_2H_5OH$ provided ethoxy 1*H*-pyrazolone **7b** and pyrazole **8b** (entry 2). However, isopropyl alcohol, isobutanol and *n*-butanol provided selectively corresponding 1*H*-pyrazolones **7c-e** (Table 5, entry 3-5). In order to evaluate the efficiency of this methodology, phenylhydrazine hydrochlorides having electron withdrawing and donating substituents **4b-g** were reacted with **2** in the presence of $Bi(OTf)_3$ in $CH_3OH$ and $C_2H_5OH$ (Table 5, entries 6-14) to give a series of corresponding 1*H*-pyrazolones **7f-o** and pyrazoles **8c-d**, **8e-j**.

**Table 5**. Preparation of alkoxymethyl 1*H*-pyrazolones **7a-o** and pyrazoles **8a-j**[a]

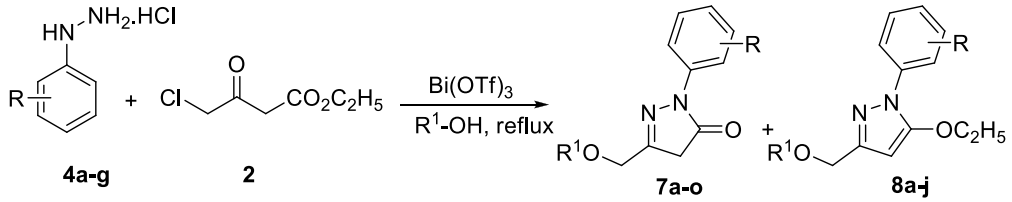


**4a-g** **2** **7a-o** **8a-j**

| S. No | Reactant **4** | R | $R^1$ | Time, (h) | Product **7** | Yield[b] (%) | Product **8** | Yield[b] (%) |
|---|---|---|---|---|---|---|---|---|
| 1 | **4a** | H | $CH_3$ | 16 | **7a** | 52 | **8a** | 15 |
| 2 | **4a** | H | $C_2H_5$ | 20 | **7b** | 45 | **8b** | 18 |
| 3 | **4a** | H | $(CH_3)_2CH$ | 18 | **7c** | 39 | **--** | -- |
| 4 | **4a** | H | $(CH_3)_2CHCH_2$ | 20 | **7d** | 36 | **--** | -- |
| 5 | **4a** | H | *n*-$C_4H_9$ | 20 | **7e** | 35 | **--** | -- |
| 6 | **4c** | *p*-F | $CH_3$ | 16 | **7f** | 56 | **8c** | 14 |
| 7 | **4e** | *p*-Br | $CH_3$ | 20 | **7g** | 54 | **8d** | 18 |
| 8 | **4f** | *p*-$OCH_3$ | $CH_3$ | 16 | **7h** | 50 | **--** | -- |
| 9 | **4d** | *p*-$CH_3$ | $CH_3$ | 18 | **7i** | 51 | **8e** | 12 |
| 10 | **4g** | *m*-Cl | $CH_3$ | 18 | **7j** | 55 | **8f** | 15 |
| 11 | **4b** | *m*-$NO_2$ | $CH_3$ | 14 | **7k** | 58 | **8g** | 10 |
| 12 | **4d** | *p*-$CH_3$ | $C_2H_5$ | 20 | **7l** | 45 | **8h** | 15 |
| 13 | **4g** | *m*-Cl | $C_2H_5$ | 18 | **7m** | 39 | **8i** | 16 |
| 14 | **4b** | *m*-$NO_2$ | $C_2H_5$ | 20 | **7n** | 51 | **8j** | 11 |
| 15 | **4g** | *m*-Cl | $(CH_3)_2CH$ | 22 | **7o** | 45 | **--** | -- |

[a] Conditions: Phenylhydrazine hydrochloride (1 mmol), ethyl 4-chloro-3-oxobutanoate (1 mmol), $Bi(OTf)_3$ (0.1 mmol), under reflux. [b] Yields of isolated products.

## CHAPTER-V

**A selective three-component, one-pot approach for the synthesis of 1,2-dihydroquinazolines and quinazolines.**

The present chapter describes the preparation of three series of compounds namely I) 1,2-dihydroquinazolines **3a-s** & **3u** II) quinazolines **5a-f** and III) Spiro cyclohexane-1,2-quinazolines **7a-d**. Three component, one-pot reaction of 2-aminoacetophenones, benzophenones with β-ketoesters and $NH_4OAc$ provided the 1,2-dihydroquinazolines. Interestingly, three component, one-pot reaction of 2-aminoacetophenones, benzophenones with ethyl 3-oxo-3-phenylpropanoate, 1,3-diketones and $NH_4OAc$ provided the quinazolines. Spiro cyclohexane-1,2-quinazolines achieved by the reaction of 2-aminoacetophenones, benzophenones with cyclohexanone and $NH_4OAc$. The combination of ammonium salts and β-ketoesters, 1,3-diketones are used for the first time to prepare these novel heterocyclic compounds.

**I) Preparation of ethyl 2-(2,4-dimethyl-1,2-dihydroquinazolin-2-yl)acetates (3a-s & 3u).**

Initially, the reaction has been carried out between 2-aminoacetophenone **1a** (1 mmol), ethyl 3-oxobutanoate **2a** (1.2 mmol) and $NH_4OAc$ (1 mmol) in $CH_3OH$ under reflux conditions (24 h) provided yellow color liquid. Based on spectral data the compound identified as ethyl 2-(2,4-dimethyl-1,2-dihydroquinazolin-2-yl)acetate **3a** (**Scheme 1**).

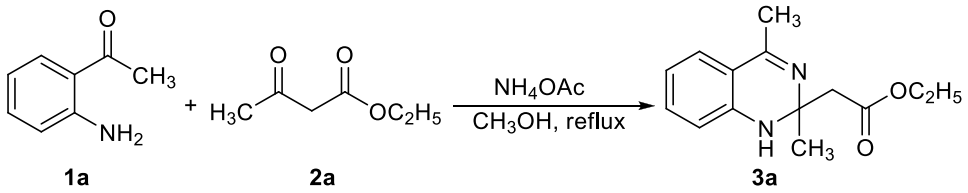


**Scheme 1**

The present method has been investigated with solvents [$CH_3OH$, $C_2H_5OH$, $CH_3CN$, THF, DCM and Toluene] and ammonium salts [$NH_4F$, $NH_4Cl$, $NH_4Br$, $NH_4NO_3$, $(NH_4)_2CO_3$ and $(NH_4)_2SO_4$]. Three equivalents of $NH_4OAc$ in the presence of $CH_3CN$ under reflux conditions produced the compound **3a** with better yield (82%). Further all these reactions have been repeated under neat conditions. These studies reveal that $NH_4OAc$ under neat conditions (100 °C) found more efficient with respect to the reaction time and yield of the product **3a** (85%; **Table 1**).

**Table 1.** Optimization of the reaction conditions.

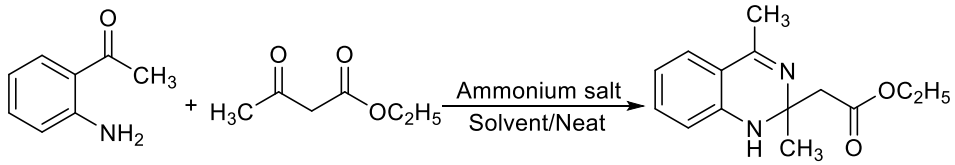


**1a** **2a** **3a**

| Entry | Ammonium salt | Equiv. | Solvent/Neat | Time (h) | Yield (%)[c] |
|---|---|---|---|---|---|
| 1 | $NH_4OAc$ | 1 | $CH_3OH$[a] | 24 | -- |
| 2 | $NH_4OAc$ | 1 | $CH_3OH$[b] | 24 | 42 |
| 3 | $NH_4OAc$ | 1 | $C_2H_5OH$[b] | 24 | 48 |
| 4 | $NH_4OAc$ | 1 | $CH_3CN$[b] | 16 | 59 |
| 5 | $NH_4OAc$ | 1 | THF[b] | 24 | 45 |
| 6 | $NH_4OAc$ | 1 | DCM[b] | 24 | 34 |
| 7 | $NH_4OAc$ | 1 | Toluene[b] | 24 | -- |
| 8 | $NH_3$ (25%) | 6 | --------[b] | 24 | 15 |
| 9 | $NH_4OAc$ | 2 | $CH_3CN$[b]/Neat | 12/3 | 68/75 |
| **10** | **$NH_4OAc$** | **3** | **$CH_3CN$[b]/Neat** | **08/3** | **82/85** |
| 11 | $NH_4OAc$ | 4 | $CH_3CN$[b]/Neat | 08/3 | 80/82 |
| 12 | $NH_4F$ | 3 | $CH_3CN$[b]/Neat | 24/4 | 58/65 |
| 13 | $NH_4Cl$ | 3 | $CH_3CN$[b]/Neat | 36/8 | 14/26 |
| 14 | $NH_4Br$ | 3 | $CH_3CN$[b]/Neat | 36/8 | 45/49 |
| 15 | $NH_4NO_3$ | 3 | $CH_3CN$[b]/Neat | 36/8 | 10/22 |
| 16 | $(NH_4)_2CO_3$ | 3 | $CH_3CN$[b]/Neat | 36/4 | 65/74 |
| 17 | $(NH_4)_2SO_4$ | 3 | $CH_3CN$[b]/Neat | 36/10 | -- |

[a] Room temperature, [b] Reflux, [c] Isolated yield, Neat (100 $^0$C)

Having optimized the reaction conditions, the present protocol extended to prepare series of 1,2-dihydroquinazolines. Accordingly, 2-aminoacetophenones **1b-c**, 2-aminobenzophenones **1d-e** were reacted with **2a-e** and $NH_4OAc$ produced the corresponding 1,2-dihydroquinazolines **3f-s**, **3u** (**Scheme 2, Fig. 1**).

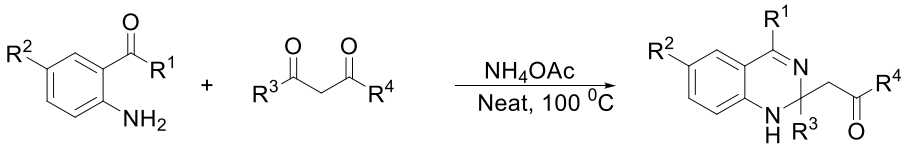


**1a-e** **2a-e** **3a-s & 3u**

**1a** $R^1 = CH_3$, $R^2 = H$ **2a** $R^3 = CH_3$, $R^4 = OC_2H_5$
**1b** $R^1 = CH_3$, $R^2 = Br$ **2b** $R^3 = CH_3$, $R^4 = O(CH_2)_2OCH_3$
**1c** $R^1 = CH_3$, $R^2 = OCH_3$ **2c** $R^3 = CH_3$, $R^4 = OCH_3$
**1d** $R^1 = Ph$, $R^2 = H$ **2d** $R^3 = CH_2Cl$, $R^4 = OC_2H_5$
**1e** $R^1 = Ph$, $R^2 = NO_2$ **2e** $R^3 = CF_3$, $R^4 = OC_2H_5$

**Scheme 2**

**1,2-dihydroquinazolines** (**3a-s & 3u**).

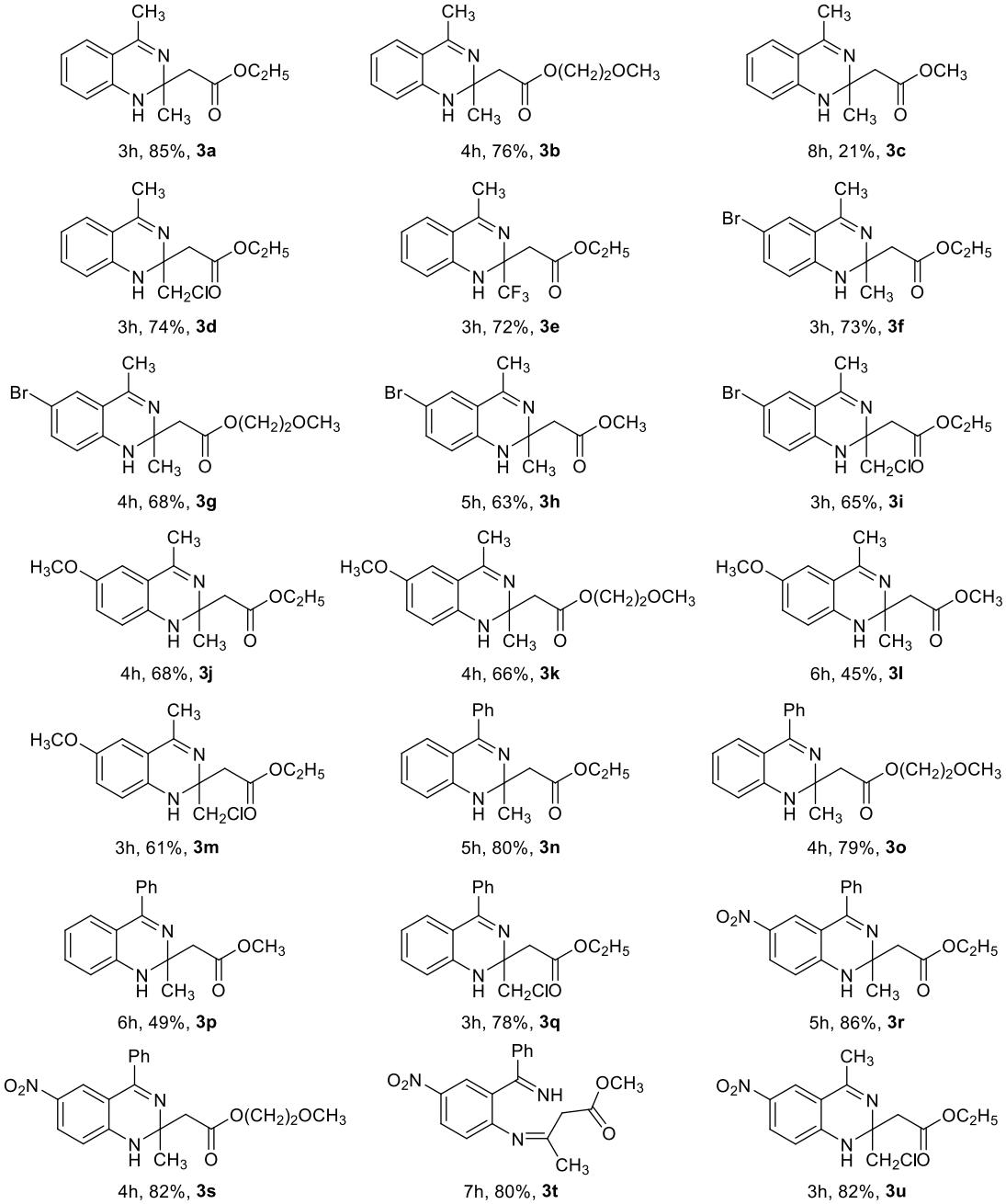


**Figure 1**

**II) Preparation of quinazolines** (**5a-f**).

The reaction of 2-aminoacetophenone **1a** (1 mmol) and ethyl 3-oxo-3-phenylpropanoate **2f** (1.2 mmol) with $NH_4OAc$ (3 mmol) has been carried out under neat conditions (100 °C, 6 h) provided the yellow solid. Based on spectral data the compound identified as 4-methyl-2-phenylquinazoline **4a** (**Scheme 3**).

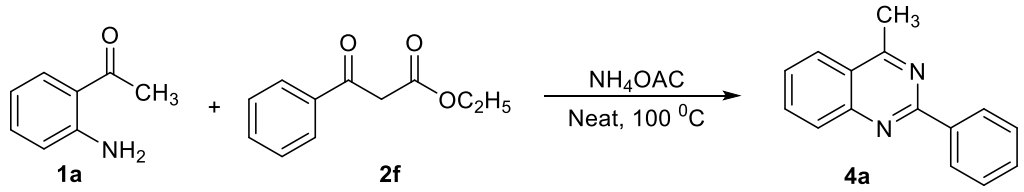


**Scheme 3**

This is an interesting reaction produced quinazoline for the first time by using β-ketoester such as ethyl 3-oxo-3-phenylpropanoate **2f**. The result encouraged us to prepare the series of quinazoline derivatives; accordingly, 2-aminoacetophenones **1b-c** and benzophenones **1d-e** were reacted with ethyl 3-oxo-3-phenylpropanoate **2f** using $NH_4OAc$ under optimized conditions. 5-Bromo-2-aminoacetophenone **1b** smoothly underwent and produced the corresponding quinazoline compound **4b**. However, 5-methoxy-2-aminoacetophenone **1c** did not work under these conditions and starting materials were recovered. Similarly, when the reaction conducted with 2-aminobenzophenone **1d** with **2f** the reaction did not provide the compound. The reaction of 5-nitro-2-aminobenzophenone **1e** and **2f** afforded the corresponding quinazoline **4c** (**Fig**. **2**).

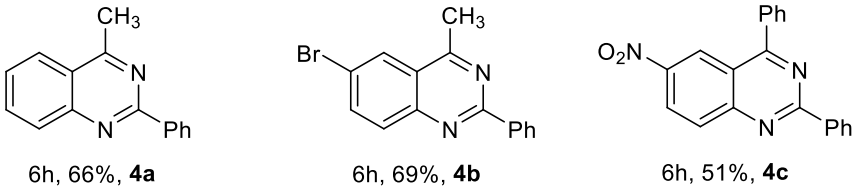


**Figure 2**

Having achieved the quinazolines with 3-oxobutanoate **2f**, further the method was extended to investigated with various 1,3-diketones. Accordingly, 2-aminoacetophenone **1a** reacted with pentane-2,4-dione **5a** under optimized condition, provided the quinazoline **4d** (**Scheme 4**). The compound **4d** was well characterized by spectral data.

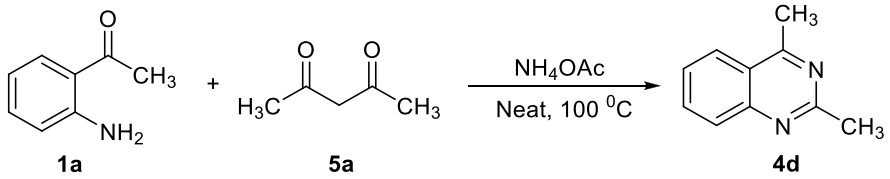


**Scheme 4**

The reactions of 2-aminoacetophenone **1b** and benzophenone **1d** carried out with pentane-2,4-dione **5a** under optimized conditions. The reactions proceeded smoothly and produced the corresponding quinazolines **4e-f** (**Fig**. **3**). Thus prepared quinazolines **4e-f** were well characterized by spectral data.

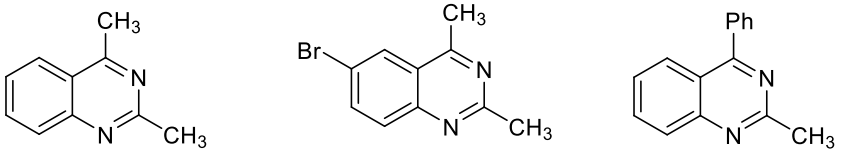


**Figure 3**

**III) Preparation of spiro cyclohexane-1,2-quinazolines** (**7a-d**).

Next, the reaction has been carried out between 2-aminoacetophenone **1a-b** and benzophenones **1d-e** (1 mmol) and cyclohexanone **6** (2 mmol) with $NH_4OAc$ (3 mmol) under neat conditions (100 °C, 3 h). This provided the spiro cyclohexane-1,2'-quinazolines **7a-d** (**Scheme 5, Fig**. **4**). The compounds **7a-d** are unknown and well characterized by spectral data.

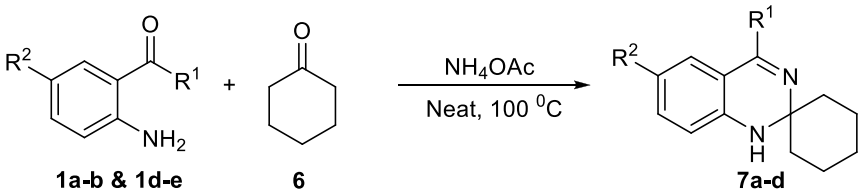


**1a** $R^1 = CH_3$, $R^2 = H$
**1b** $R^1 = CH_3$, $R^2 = Br$
**1d** $R^1 = Ph$, $R^2 = H$
**1e** $R^1 = Ph$, $R^2 = NO_2$

**Scheme 5**

**Spiro cyclohexane-1,2-quinazolines** (**7a-d**).

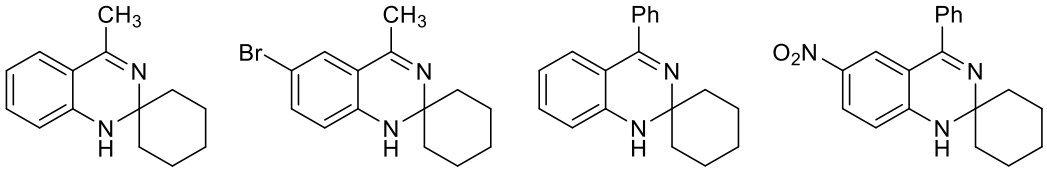


**Figure 4**